Vanishing capillarity solutions of Buckley-Leverett equation with gravity in two-rocks' medium.

Boris Andreianov[*]   Clément Cancès[†]

Abstract

For the hyperbolic conservation laws with discontinuous flux function there may exist several consistent notions of entropy solutions; the difference between them lies in the choice of the coupling across the flux discontinuity interface. In the context of Buckley-Leverett equations, each notion of solution is uniquely determined by the choice of a "connection", which is the unique stationary solution that takes the form of an undercompressive shock at the interface. To select the appropriate connection, following Kaasschieter [39] one may use the parabolic model with small parameter that accounts for capillary effects. While it has been recognized in [26] that the "optimal" connection and the "barrier" connection may appear at the vanishing capillarity limit, in this paper we show that any connection may appear. We give a simple procedure that permits to determine the appropriate connection in terms of the flux profiles and capillary pressure profiles present in the model. This information is used to construct a finite volume numerical method for the Buckley-Leverett equation with interface coupling that retains information from the vanishing capillarity model. We illustrate the theoretical result with numerical examples.

Keywords   scalar conservation laws with discontinuous flux functions, two-phase flows in heterogeneous porous media, finite volume schemes

AMS classification (2010)   35L02, 35L65, 65M08, 76S05

Contents

[*]boris.andreianov@univ-fcomte.fr
[†]cances@ann.jussieu.fr

Introduction

The Buckley-Leverett equation is a scalar conservation law

$$\partial_t s + \partial_x f(x, s) = 0$$

with a particular form of the flux function $f(x, \cdot)$; the dependence in x describes the medium heterogeneities, and the whole equation serves as a model for two-phase immiscible flow in one-dimensional medium with neglected capillarity effects. The details of the models (with and without capillarity) are recalled in the sequel. When the dependence of f on x is regular, the notion of Kruzhkov entropy solution [40] has been recognized as the appropriate one; in particular, it is known that, whatever be the form of the capillary pressure curves, the "vanishing capillarity limit" yields the Kruzhkov solution (e.g., in the autonomous case, one can deduce this convergence result from the approach of [15]; for the general case, the result of [46] can be used). The situation is much more delicate when the medium consists of two or more geological layers with radically different physical properties and a sharp transition between the layers; mathematically, this means that $x \mapsto f(x, \cdot)$ presents discontinuities. Several works were devoted to the study of such *discontinuous-flux Buckley-Leverett model*; let us mention Gimse and Risebro [37, 38], Kaasschieter [39], Adimurthi et al. [1, 2], Bürger et al. [19] (see also [20]), and the works [24, 25, 26] of the second author. These works were mainly considering the model problem with interface located at $x = 0$ and piecewise constant in x flux $f(x, \cdot) = f_L(\cdot)\mathbb{1}_{x<0} + f_R(\cdot)\mathbb{1}_{x>0}$; this will also be our framework in this paper.

In particular, Adimurthi, Mishra and Veerappa Gowda in [2] have pointed out the fact that infinitely many notions of solution, all of them equally consistent from the mathematical point of view, may coexist for the discontinuous-flux Buckley-Leverett equation; this fact was illustrated numerically in [19]. The so-called "optimal entropy solutions" (here and in the sequel, we follow the terminology of [24, 25, 26]) were recognized as the vanishing capillarity limits (with discontinuous capillarity $\pi(x, \cdot) = \pi_L(\cdot)\mathbb{1}_{x<0} + \pi_R(\cdot)\mathbb{1}_{x>0}$) in some physical situations: see [39, 1, 24]. In [25], it was shown that the so-called "barrier entropy solutions" appear, in another physical range of parameters. Roughly speaking, the optimal entropy solutions correspond to the maximization of the flux of one phase across the interface while the barrier entropy solutions correspond to the situation where the flux of this same phase across the interface is minimized (cf. [26]). As shown in [25], the occurrence of the barrier entropy solution can be linked to the *oil trapping* phenomenon. In this paper we show, both theoretically and numerically, that all intermediate notions of entropy solutions, described by Adimurthi, Mishra and Veerappa Gowda in [2] and by Bürger, Karlsen and Towers in [20], do appear as vanishing capillarity limits. More importantly, we indicate a simple procedure that permits to identify the adequate notion of solution, given the graphs of the flux functions $f_{L,R}$ and of the capillarity functions $\pi_{L,R}$.

While the starting point of our analysis is exactly the same as in the work of Kaasschieter [39], we exploit the theoretical framework of the paper [7] of Karlsen, Risebro and the first author (see also Bürger et al. [20]) in order to avoid the lengthy analysis of vanishing capillarity profiles corresponding to different Riemann data. Namely, from the facts established in [2, 20, 7] and those assessed in [23, 28], we deduce that only one vanishing capillarity profile should be constructed explicitly. The choice of the profile follows a simple geometrical rule (see Fig. 1 and Proposition 3).

The paper is organized as follows. In Section 1, we recall the parabolic model for two-rocks' porous medium, and the notions of bounded-flux and mild solutions as introduced in [28]. The key point here is the so-called Kato inequality, which is a localized L^1 contraction principle satisfied by two mild solutions. In Section 1.3, we point out a particular mild solution; this is a viscosity profile connecting some states (s_L^π, s_R^π) defined from transmission conditions across the interface. This profile gives rise to the particular stationary solution $c(x) = s_L^\pi \mathbb{1}_{x<0} + s_R^\pi \mathbb{1}_{x>0}$ for the hyperbolic Buckley-Leverett model in two-rocks' medium described in Section 2. Namely, $c(\cdot)$ can be obtained as a vanishing capillarity limit, therefore it must be considered as an admissible solution for the hyperbolic model. Using this fact and the general structure of entropy solutions to our hyperbolic model, in Theorem 5 we eventually identify the vanishing capillarity limits as the $\mathcal{G}_{(s_L^\pi, s_R^\pi)}$-entropy solutions in the sense of [7]. Finally, in Section 3 we illustrate numerically the above theoretical results. For solving the hyperbolic model obtained as the vanishing capillarity limit, we use a simple finite volume Godunov scheme designed in [4] to approximate the discontinuous-flux Buckley-Leverett equation in a way compatible with the more precise parabolic model with capillarity. In order to illustrate the efficiency of the procedure, we compare the results provided by this Godunov scheme with those provided by the scheme (analyzed in [23]) that approximates the parabolic problem. In particular, we observe a remarkable computational gain in considering the simplified model, as well as a good concordance in the numerical results.

1 Parabolic model for two-phase flow in two-rocks' medium

This section is devoted to the parabolic model of two-phase flow with discontinuous capillary pressure in one space dimension. Following the previous work of the second author [28, 23, 29] (see also [47, 21]), the frame of multivalued capillary pressures is introduced in order to give a extended sense to the continuity of the capillary pressure at the medium's discontinuity. We will use the notions of bounded-flux and mild solutions that have been proved to be well-suited for this problem in [28, 23]. This model will be re-scaled, letting a scaling parameter appear in front of the capillary diffusion. Letting the capillarity parameter ϵ tend to zero will be the main purpose of this paper, and especially of Section 2.2.

1.1 Immiscible two-phase flows with discontinuous capillary pressure

We consider a one-dimensional porous medium made of two different rocks $\Omega_L = (-\infty, 0)$ and $\Omega_R = (0, +\infty)$, separated by an interface $\Gamma = \{x = 0\}$. The medium is assumed to be vertical, but we use the subscripts L ("Left") for the lower rock, and R ("Right") for the upper rock in order to comply with the notation used in the context of conservation laws with discontinuous flux. Two immiscible and incompressible phases a, b are flowing within this medium. Writing the volume balance of each phase in Ω_i yields

$$\phi_i \partial_t s_\alpha + \partial_x v_\alpha = 0 \qquad (\alpha \in \{a, b\}, i \in \{L, R\}), \tag{1}$$

where $s_\alpha \in [0, 1]$ denotes the saturation of the phase α and $\phi_i \in (0, 1)$ denotes the porosity of the rock Ω_i. The filtration speed v_α of the phase α is prescribed by the Darcy-Muskat law (see e.g. [13])

$$v_\alpha = -K_i \frac{kr_{\alpha,i}(s_\alpha)}{\mu_\alpha} (\partial_x p_\alpha - \rho_\alpha g) \qquad (\alpha \in \{a, b\}, i \in \{L, R\}), \tag{2}$$

where K_i is the intrinsic permeability of Ω_i, μ_α, p_α and ρ_α are respectively the viscosity, the pressure and the density of the phase α, and g is the gravity. Whenever $\rho_a \neq \rho_b$, the presence of gravity induces the buoyancy force. The relative permeability $kr_{\alpha,i}$ of the phase α in Ω_i is supposed to be Lipschitz continuous, increasing on $[0, 1]$ and such that $kr_{\alpha,i}(0) = 0$. The pore volume is supposed to be fully saturated by the fluid, i.e.

$$s_a + s_b = 1, \tag{3}$$

while the phase pressures are supposed to be linked by the capillary pressure relation

$$p_a - p_b = \pi_i(s_a), \qquad (i \in \{L, R\}), \tag{4}$$

where the functions π_i are increasing. As noticed by H. W. Alt *et al.* [3], the natural topology for the phase pressure p_α stems from the estimate

$$\sum_i \int_{\Omega_i} kr_{\alpha,i}(s_\alpha) (\partial_x p_\alpha)^2 \, dx \leq C. \tag{5}$$

Therefore, if $s_\alpha = 0$ (and thus $kr_{\alpha,i}(s_\alpha) = 0$), no control is provided by (5) on the pressure p_α. As suggested in [29] (see also [17, 16]), we extend the pressure in the following multivalued way

$$p_a(x, t) = [-\infty, p_b(x, t) + \pi_i(0)] \qquad \text{if } x \in \Omega_i \text{ and } s_a(x, t) = 0, \tag{6a}$$
$$p_b(x, t) = [-\infty, p_a(x, t)) - \pi_i(1)] \qquad \text{if } x \in \Omega_i \text{ and } s_a(x, t) = 1, \tag{6b}$$

for $i = L, R$. Therefore, as it was already the case in [21, 28], the capillary pressure function has to be extended into the maximal monotone graph $\tilde{\pi}_i$ from $[0, 1]$ to $[-\infty, +\infty]$ defined by

$$\tilde{\pi}_i(s) = \begin{cases} \pi_i(s) & \text{if } s \in (0, 1), \\ [-\infty, \pi_i(0)] & \text{if } s = 0, \\ [\pi_i(1), +\infty] & \text{if } s = 1. \end{cases} \tag{7}$$

At the interface Γ, we require the balance of the phase fluxes, i.e. (formally)

$$v_\alpha(0^-, t) = v_\alpha(0^+, t) \qquad (\alpha \in \{a, b\}), \tag{8}$$

and the continuity of the extended phase pressures, i.e.

$$p_\alpha(0^-, t) \cap p_\alpha(0^+, t) \neq \emptyset. \tag{9}$$

Here and at the sequel, the values at $x = 0^\pm$ denote the one-sided traces of different quantities, in some sense that has to be made precise in each case.

Now, summing (1) for $\alpha = a, b$ we find that $\partial_x(v_a + v_b) = 0$. Thanks to (8), we can claim that the total flow rate $q := v_a + v_b$ only depends on time. For the sake of simplicity, we assume that q is constant in time. However, our results can be generalized to the case of time dependent q by means of an adaptation of the tools developed in [6, 5, 22]. Without loss of generality, we assume that $q \geq 0$ and that the buoyancy coefficient $(\rho_a - \rho_b)g$ is nonnegative (these conditions can be enforced by changing x by $-x$ and by exchanging the role of a and b). The equation (1) for the phase a can now be rewritten under the form

$$\phi_i \partial_t s_a + \partial_x \left(f_i(s_a) - \lambda_i(s_a) \partial_x \pi_i(s_a) \right) = 0, \tag{10}$$

where, for $i = L, R$,

$$\lambda_i(s) = K_i \frac{kr_{a,i}(s) kr_{b,i}(1-s)}{\mu_b kr_{a,i}(s) + \mu_a kr_{b,i}(1-s)}, \quad f_i(s) = q \frac{kr_{a,i}(s)}{kr_{a,i}(s) + \frac{\mu_a}{\mu_b} kr_{b,i}(1-s)} + (\rho_a - \rho_b)g\lambda_i(s). \tag{11}$$

Since we assumed that $kr_{a,i}(s), kr_{b,i}(s)$ are zero if and only if $s = 0$, the functions λ_i verify $\lambda_i(0) = \lambda_i(1) = 0$ and $\lambda_i(s) > 0$ if $s \in (0,1)$, while the functions f_i are such that $f_i(0) = 0$ and $f_i(1) = q$. For classical choices of relative permeabilities $kr_{a,i}$ and $kr_{b,i}$ (see e.g. [13]), the flux functions f_i, $i = L, R$, are *bell-shaped* in the sense (**A1**) below.

For the sake of readability, we remove the index a in s_a; thus s stands for the saturation of the phase a. Denoting by φ_i the Kirchhoff's transform function defined by

$$\varphi_i(s) = \int_0^s \lambda_i(z) \pi_i'(z) dz,$$

we convert equation (11), valid in Ω_i, into

$$\phi_i \partial_t s + \partial_x \left(f_i(s) - \partial_x \varphi_i(s) \right) = 0. \tag{12}$$

Thus equation (8) becomes

$$\lim_{x \to 0^-} \left(f_L(s) - \partial_x \varphi_L(s) \right) = \lim_{x \to 0^+} \left(f_R(s) - \partial_x \varphi_R(s) \right); \tag{13}$$

the precise sense of equality (13) will be specified later. Notice that traces at $x = 0^\pm$ of $\varphi_i(s)$ exist whenever $\varphi_i(s(t, \cdot)) \in H^1(\Omega_i)$. Since each φ_i admits a continuous inverse function, also the one-sided traces of s on Γ exist in the strong $L^1(0,T)$ sense. Denote by s_L, s_R the traces on Γ from Ω_L and Ω_R respectively; it has been shown in [21, 28, 29] that relation (9) implies

$$\tilde\pi_L(s_L) \cap \tilde\pi_R(s_R) \neq \emptyset. \tag{14}$$

Note that in this paper, buoyancy is taken into account, and, as it will be stressed in the sequel, it plays a major role in the following study. Indeed, it makes the flux f_i defined by (11) *bell-shaped* in the sense of assumption (**A1**) below. In the case where the gravity was neglected, existence of traveling wave solutions to problem (12)–(14) was investigated in [50], while existence and uniqueness of (regular) weak solutions was shown in [14, 28, 47]. The effective equations in a stratified porous medium were formally derived in [49], and rigorously recovered in [47]. Numerical schemes were proposed in [36, 1, 35] and analyzed in [34]. To our knowledge, the only results available concerning the analysis of problem (12)–(14) in presence of gravity are [39] for the traveling waves and [23] for the existence and uniqueness of the solutions, existence being proved by establishing the convergence of a suitable finite volume scheme. Multi-dimensional extensions have been recently performed [29, 17, 16].

Due to the large dimensions of the sedimentary basins, and since the time scale involved in the migration of hydrocarbons is also large, it is natural to rescale the variables by choosing $x := x/\epsilon$, $t := t/\epsilon$ for some small positive ϵ. The problem (12)–(14), completed with the initial condition (15d), thus turns into

$$\phi_i \partial_t s^\epsilon + \partial_x \left(f_i(s^\epsilon) - \epsilon \partial_x \varphi_i(s^\epsilon) \right) = 0 \quad \text{in } \Omega_i \times (0, \infty), \tag{15a}$$

$$\lim_{x \to 0^-} \left(f_L(s^\epsilon) - \epsilon \partial_x \varphi_L(s^\epsilon) \right) = \lim_{x \to 0^+} \left(f_R(s^\epsilon) - \epsilon \partial_x \varphi_R(s^\epsilon) \right) \quad \text{in } (0, T), \tag{15b}$$

$$\tilde\pi_L(s_L^\epsilon) \cap \tilde\pi_R(s_R^\epsilon) \neq \emptyset \quad \text{in } (0, T), \tag{15c}$$

$$s^\epsilon_{|t=0} = s_0 \quad \text{in } \mathbb{R}. \tag{15d}$$

Here, as usual, $i = L, R$ and s_L^ϵ, s_R^ϵ denote the traces of s^ϵ at $x = 0^-$ and $x = 0^+$, respectively. The flux transmission property (15b) should be understood in the weak sense, e.g., according to the theory of [32].

Let us now make precise the assumptions on the data required for our analysis. It is worth noting that all of them are fulfilled by the model commonly used in oil-engineering (see [13, 9]).

(A1) The flux functions f_i belong to $\mathrm{Lip}([0,1])$ and satisfy $f_i(0) = 0, f_i(1) = q \geq 0$. Moreover, f_i is a so-called *bell-shaped* function, i.e. there exists $\overline{s}_i \in (0,1]$ such that $f_i'(s)(\overline{s}_i - s) > 0$ for a.e. $s \in (0,1)$.

(A2) The capillary pressure functions π_i belong to $\mathrm{Lip}_{loc}((0,1)) \cap L^1((0,1))$ and they are strictly increasing on $(0,1)$.

(A3) The Kirchhoff transforms φ_i belong to $\mathrm{Lip}([0,1])$ and they are strictly increasing on $[0,1]$.

(A4) s_0 is measurable with $0 \leq s_0 \leq 1$.

Hereabove, $i = L, R$; and by Lip and Lip_{loc} we denote the spaces of Lipschitz and locally Lipschitz continuous functions, respectively.

1.2   Bounded-flux solutions and mild solutions of (15)

The mathematical analysis of the system (15) for fixed ϵ is carried out in [14, 47, 28] in cases where the gravity (and thus the buoyancy) is neglected, and in [23] in presence of buoyancy. Let us recall the framework of *bounded-flux solutions* introduced in [28, 23] for this problem.

Definition 1 (bounded-flux solution) *A function $s^\epsilon \in L^\infty(\mathbb{R} \times \mathbb{R}_+; [0,1])$ is said to be a* bounded flux solution *of problem* (15) *with initial datum s_0 if $\partial_x \varphi_i(s^\epsilon) \in L^\infty(\Omega_i \times \mathbb{R}_+)$, if $\tilde{\pi}_L(s_L^\epsilon(t)) \cap \tilde{\pi}_R(s_R^\epsilon(t)) \neq \emptyset$ for a.e. $t \in \mathbb{R}_+$, and if, for all $\psi \in \mathcal{C}_c^\infty(\mathbb{R} \times \mathbb{R}_+)$,*

$$\iint_{\mathbb{R} \times \mathbb{R}_+} \phi_i s^\epsilon \partial_t \psi + \int_\mathbb{R} \phi_i s_0 \psi(\cdot, 0) + \sum_{i \in \{L,R\}} \iint_{\Omega_i \times \mathbb{R}_+} (f_i(s^\epsilon) - \epsilon \partial_x \varphi_i(s^\epsilon)) \partial_x \psi = 0. \tag{16}$$

From now on, we use the *semi-Kruzhkov entropy fluxes*

$$\Phi_i^\pm(a,b) = \mathrm{sign}_\pm(a-b)(f_i(a) - f_i(b)),$$

where $\mathrm{sign}_+(a) = 1$ if $a > 0$ and 0 otherwise, and $\mathrm{sign}_-(a) = -\mathrm{sign}_+(-a)$. In the sequel, for $a \in \mathbb{R}$, we denote by a^+ (resp. a^-) the positive (resp. negative) part of a, i.e. $a^\pm = \mathrm{sign}_\pm(a)a$.

Proposition 1 *Let $s^\epsilon, \check{s}^\epsilon$ be two bounded-flux solutions of* (15) *in the sense of Definition 1 corresponding to initial data $s_0, \check{s}_0$ respectively. Then for all $\psi \in \mathcal{C}_c^\infty(\mathbb{R} \times \mathbb{R}_+; \mathbb{R}+)$, the following Kato inequality holds:*

$$\sum_{i \in \{L,R\}} \iint_{\Omega_i \times \mathbb{R}_+} \phi_i(s^\epsilon - \check{s}^\epsilon)^\pm \partial_t \psi + \sum_{i \in \{L,R\}} \int_{\Omega_i} \phi_i(s_0 - \check{s}_0)^\pm \psi(\cdot, 0)$$
$$+ \sum_{i \in \{L,R\}} \iint_{\Omega_i \times \mathbb{R}_+} \left(\Phi_i^\pm(s^\epsilon, \check{s}^\epsilon) - \epsilon \partial_x (\varphi_i(s^\epsilon) - \varphi_i(\check{s}^\epsilon))^\pm \right) \partial_x \psi \geq 0. \tag{17}$$

Corollary 2 *For all initial datum s_0 satisfying* **(A4)** *there exists at most one bounded-flux solution s^ϵ to* (15).

If we consider L^1 data with values in $[0,1]$, then we can adapt the proof proposed in [28] as suggested in [24], the L^1 assumption being used to ensure that $\partial_x \varphi_{L,R}(s) \to 0$ as $x \to \pm\infty$. For the general case, let us point out that the L^1 assumption is bypassed, e.g., by exploiting the Kato inequality in the way of Maliki and Touré [42]. Thus **(A4)** is a sufficient assumption in Corollary 2.

Theorem 1 *Assume that* **(A1)**–**(A4)** *hold. In addition, let the initial datum be regular in the sense*

(A5) *for $i = L, R$, assume $\partial_x \varphi_i(s_0) \in L^\infty(\Omega_i)$. Furthermore, assume that the initial data are connected; namely, denoting by $s_{0,i}$ the trace of s_0 on Γ from Ω_i, we suppose that $\tilde{\pi}_L(s_{0,L}) \cap \tilde{\pi}_R(s_{0,R}) \neq \emptyset$.*

*Then there exists a unique bounded-flux solution s^ϵ of problem (15) corresponding to s_0. Furthermore, s^ϵ belongs to $\mathcal{C}(\mathbb{R}_+; L^1_{\mathrm{loc}}(\mathbb{R}))$. Moreover, if $\check{s}_0$ also satisfies **(A4)** and **(A5)**, if $s_0 - \check{s}_0 \in L^1(\mathbb{R})$ and if we denote by $\check{s}^\epsilon$ the unique bounded-flux solution corresponding to $\check{s}_0$, then for all $t \geq 0$ we have*

$$\sum_{i \in \{L,R\}} \int_{\Omega_i} \phi_i \left(s^\epsilon(\cdot,t) - \check{s}^\epsilon(\cdot,t)\right)^\pm \leq \sum_{i \in \{L,R\}} \int_{\Omega_i} \phi_i \left(s_0(x) - \check{s}_0(x)\right)^\pm. \tag{18}$$

Upon generalizing the notion of solution by a closure procedure, the above existence and uniqueness framework can be extended to initial data that only satisfy **(A4)**, but not **(A5)**.

Definition 2 (mild solution) *A function $s^\epsilon \in L^\infty(\mathbb{R} \times \mathbb{R}_+; [0,1])$ is said to be a* mild solution *if for $i = L, R$, $\partial_x \varphi_i(s^\epsilon) \in L^2_{loc}(\bar{\Omega}_i \times \mathbb{R}_+)$, if $\tilde{\pi}_L(s^\epsilon_L(t)) \cap \tilde{\pi}_R(s^\epsilon_R(t)) \neq \emptyset$ for a.e. $t \in \mathbb{R}_+$, and if there exists a sequence $(s^{\nu,\epsilon})_\nu$ of bounded flux solutions tending towards s^ϵ in $L^1_{loc}(\mathbb{R} \times \mathbb{R}_+)$.*

The following result is essentially contained in [28, 23].

Theorem 2 *Assume that **(A1)**–**(A4)** hold, then there exists a unique* mild solution s^ϵ *of (15) corresponding to s_0. Furthermore, s^ϵ belongs to $\mathcal{C}(\mathbb{R}_+; L^1_{\mathrm{loc}}(\mathbb{R}))$. Moreover, if $\check{s}^\epsilon$ is a mild solution corresponding to an initial datum $\check{s}_0$ then the Kato inequality (17) holds.*

Proof: Let us start with the case of a compactly supported initial datum. In this case, smoothing s_0 and modifying it near the origin as proposed in [24, 25], we can approximate s_0 in $L^1(\mathbb{R})$ by a sequence $(s_0^\nu)_{\nu \in \mathbb{N}}$ of initial data that are regular in the sense **(A5)**. Denoting by $s^{\nu,\epsilon}$ the unique bounded-flux solution corresponding to the initial data s_0^ν, we see from (18) that the sequence $(s^{\nu,\epsilon})_\nu$ is a Cauchy sequence in $\mathcal{C}(\mathbb{R}_+; L^1(\mathbb{R}))$ Therefore, it admits a unique limit value s^ϵ.

Let us show that s^ϵ is a mild solution. Let $\mathcal{K}$ be an arbitrary bounded interval of $\mathbb{R}$, let $T > 0$, and let $\chi_i : \overline{\Omega}_i \to [0,1]$ be a smooth function with compact support such that $\chi_i \equiv 1$ on Ω_i. Choosing formally

$$(x,t) \mapsto \pi(x, s^{\nu,\epsilon}(x,t)) \mathbb{1}_{(0,T)}(t) \chi_i(x)$$

as test function in the weak formulation (16) on $s^{\nu,\epsilon}$ (this point is thoroughly justified, by the mean of two steps of regularization of the problem in [28] — see also [29] for the multidimensional case) provides that

$$\epsilon \int_0^T \sum_{i \in \{L,R\}} \int_{\mathcal{K}_i} (\partial_x \varphi_i(s^{\nu,\epsilon}))^2 \leq C, \tag{19}$$

where $\mathcal{K}_i = \mathcal{K} \cap \Omega_i$ and where C does not depend on ν nor on ϵ (but on $\mathcal{K}$). Then $\varphi_i(s^{\nu,\epsilon})$ is uniformly bounded in $L^2((0,T); H^1(\mathcal{K}_i))$ with respect to ν. Since $\varphi_i(s^{\nu,\epsilon})$ converges strongly towards $\varphi_i(s^\epsilon)$ in $\mathcal{C}([0,T]; L^2(\mathcal{K}_i))$, by interpolation, it also converges strongly in $L^2((0,T); H^s(\mathcal{K}_i))$ (to the same limit) as soon as $s < 1$. Hence, we infer the strong convergence of the one-sided traces $\varphi_i(s_i^{\nu,\epsilon})$ on the interface in the $L^2(0,T)$ sense towards $\varphi_i(s_i^\epsilon)$. The functions φ_i^{-1} being invertible, we deduce that $s_i^{\nu,\epsilon}$ tends to s_i^ϵ. Since the set $\{(s_L, s_R) \in [0,1]^2 \mid \tilde{\pi}_L(s_L) \cap \tilde{\pi}_R(s_R) \neq \emptyset\}$ is closed, one recovers at the limit $\nu \to \infty$ the property $\tilde{\pi}_L(s_L^\epsilon) \cap \tilde{\pi}_R(s_R^\epsilon) \neq \emptyset$ a.e. in $(0,T)$, and then a.e. in $\mathbb{R}_+$ since T has been chosen arbitrary. This ends the existence proof for compactly supported data.

Next, given a general initial datum s_0, we can approximate it by a monotone sequence $(s_0^m)_{m \in \mathbb{N}}$ by setting $s_0^m := s_0 \mathbb{1}_{|x|<m}$. Using the comparison principle contained in (18), we see that the corresponding sequence $(s^{m,\epsilon})$ of mild solutions is non-decreasing, then it converges to some limit s^ϵ a.e. on $\mathbb{R} \times [0,T]$. It follows that s^ϵ is itself a mild solution.

Finally, mild solutions being constructed as L^1_{loc} limits of bounded-flux solutions, the Kato inequality (17) remains true because it is stable by L^1_{loc} convergence. A mild solution is a weak solution, i.e. it satisfies (16); therefore, we deduce from [27] that s^ϵ belongs to $\mathcal{C}([0,T]; L^1_{loc}(\Omega_i))$. Since $s^\epsilon \in L^\infty(\mathbb{R} \times \mathbb{R}_+)$, one obtains that $s^\epsilon \in \mathcal{C}([0,T]; L^1_{loc}(\mathbb{R}))$. $\square$

As a consequence of the Kato inequality, the comparison and L^1-contraction property (18) remains valid for mild solution instead of bounded-flux solution. Last but not least, all the equations of system (15) are still fulfilled, in the distributional sense or in the appropriate trace sense, by the mild solutions, ensuring that they are effective solutions to the problem. To sum up, Theorem 2 sets up a well-posedness framework for (15), for all $\epsilon > 0$.

1.3 Looking for a stationary profile solution

Clearly, ϵ in (15) can be seen as a vanishing capillarity parameter. In order to understand the limit problem, as $\epsilon \to 0$, in this paragraph we point out an evident stationary profile $U : \mathbb{R} \mapsto [0,1]$ such that for all ϵ, $U(x/\epsilon)$ yields a bounded-flux solution to problem (15). In the simplest case, U is constant on each side from zero; in the other case, U is constant on one side only.
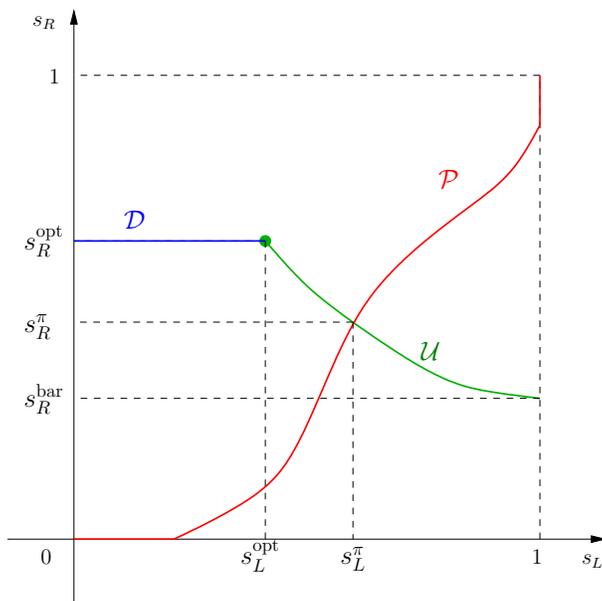

Figure 1: The maximal monotone graph $\mathcal{P}$ (in red) is defined by (20) from the capillary pressure function $\pi_{L,R}$, and the decreasing curve $\mathcal{U}$ (in green) is defined by (21) from the convective flux functions $f_{L,R}$. The vanishing capillarity limit is fully characterized by their intersection, as stated in the "selection rule" at the end of the section. The segment $\mathcal{D}$ (horizontal, in the case $s_L^{opt} = \bar{s}_L$) is used in the proof of Prop. 3.

Given $\pi_{L,R}$ and $f_{L,R}$, we define two curves $\mathcal{P}$ and $\mathcal{U}$ in the unit square $[0,1] \times [0,1]$ (see Fig. 1). Recall that we have extended $\pi_{L,R}$ to maximal monotone graphs $\tilde{\pi}_{L,R}$ from $[0,1]$ to $\bar{\mathbb{R}}$, thus extending the domain of $\pi_{L,R}^{-1}$ to whole $\bar{\mathbb{R}}$ (the inverse of a maximal monotone graph is a maximal monotone graph). Define the set

$$\mathcal{P} := \left\{ (s_L, s_R) \in [0,1]^2 \mid \tilde{\pi}_L(s_L) \cap \tilde{\pi}_R(s_R) \neq \emptyset \right\}, \tag{20}$$

then the curve $\mathcal{P}$ is the maximal monotone graph from $[0,1]$ to $[0,1]$ defined as the composition $\tilde{\pi}_R^{-1} \circ \tilde{\pi}_L$ of two maximal monotone graphs. The curve $\mathcal{U}$ is implicitly given by

$$\mathcal{U} := \left\{ (s_L, s_R) \mid f_L(s_L) = f_R(s_R), \ \ s_L \geq \bar{s}_L \ \text{ and } \ s_R \leq \bar{s}_R \right\}. \tag{21}$$

Due to assumption (**A1**), $\mathcal{U}$ is the graph of a strictly decreasing function on an interval that we denote $[s_L^{opt}, s_L^{bar}]$. More specifically, the extremity (s_L^{opt}, s_R^{opt}) of the curve $\mathcal{U}$ lies inside $(0,1)^2$; we have either $s_L^{opt} = \bar{s}_L$ or $s_R^{opt} = \bar{s}_R$ according to the order of the values $\max_{[0,1]} f_L$ and $\max_{[0,1]} f_R$. The other extremity (s_L^{bar}, s_R^{bar}) lies either on the part $\{1\} \times [0, s_R^{opt}]$ or on the part $[s_L^{opt}, 1] \times \{0\}$ of the boundary of the unit square, according to the sign of the total flux q.

Proposition 3
(i) Assume that $\mathcal{U} \cap \mathcal{P} \neq \emptyset$, and denote by (s_L^π, s_R^π) its unique element. Then $c(x) := s_L^\pi \mathbb{1}_{x<0} + s_R^\pi \mathbb{1}_{x>0}$ is a bounded-flux solution of (15) for every $\epsilon > 0$, it is therefore a vanishing capillarity limit.
(ii) Assume that $\mathcal{U} \cap \mathcal{P} = \emptyset$. Then $c(x) := s_L^{opt} \mathbb{1}_{x<0} + s_R^{opt} \mathbb{1}_{x>0}$ is a vanishing capillarity limit, i.e., there exists a sequence of stationary bounded-flux solutions of (15) that converges to $c(\cdot)$ in $L^1_{loc}(\mathbb{R})$, as $\epsilon \to 0$.

In the above statement, saying that a function is a solution of (15) we do not specify the initial condition.

Proof:

(i) It is enough to check that the function $c(\cdot)$ fits the definition of a bounded-flux solution. Indeed, it is constant on each side of the interface, so that the equation is verified pointwise away from $\{x = 0\}$. Next, the capillary pressures are connected in the sense $\pi_L(s_L^\pi) \cap \pi_R(s_R^\pi) \neq \emptyset$ because $(s_L^\pi, s_R^\pi) \in \mathcal{P}$. Finally, because $(s_L^\pi, s_R^\pi) \in \mathcal{U}$, we have

$$(f_L(c) - \epsilon\partial_x c)|_{x=0^-} = f_L(s_L^\pi) = f_R(s_R^\pi) = (f_R(c) - \epsilon\partial_x c)|_{x=0^+}.$$

(ii) The proof in this case is similar to the proof of [24, Proposition 2.9], in which a particular choice of $\mathcal{P}$ was done. We consider separately two cases: either $s_L^{opt} = \bar{s}_L$, or $s_R^{opt} = \bar{s}_R$. In the first case we complement $\mathcal{U}$ by the horizontal segment $\mathcal{D} := [0, s_L^{opt}] \times \{s_R^{opt}\}$ (see Fig. 1); in the second case we complement $\mathcal{U}$ by the vertical segment $\mathcal{D} := \{s_L^{opt}\} \times [s_R^{opt}, 1]$. In each of the cases, there is an intersection point $(\widetilde{s}_L^\pi, \widetilde{s}_R^\pi)$ of the maximal monotone graph $\mathcal{P}$ with the union $\mathcal{U} \cup \mathcal{D}$ which is a maximal anti-monotone graph. Since $\mathcal{U} \cap \mathcal{P} = \emptyset$ by assumption, the point $(\widetilde{s}_L^\pi, \widetilde{s}_R^\pi)$ belongs to $\mathcal{D}$.

Consider the first case: we have $\widetilde{s}_R^\pi = s_R^{opt}$, $\widetilde{s}_L^\pi < s_L^{opt}$, and $f_L(\cdot) - f_L(s_L^{opt}) \leq 0$ on $[0, 1]$. We construct the solution of the following Cauchy problem for the ordinary differential equation:

$$\begin{cases} \lambda_L(U(\xi)) \left[\pi_L(U(\xi))\right]' = f_L(U(\xi)) - f_L(s_L^{opt}), & \xi \in (-\infty, 0] \\ U(0) = \widetilde{s}_L^\pi. \end{cases} \tag{22}$$

Existence of a local solution is clear from the Cauchy-Peano theorem, and it is easily seen that the solution is non-increasing and it can be continued to a global on $(-\infty, 0]$ solution satisfying $\lim_{\xi \to -\infty} U(\xi) = s_L^{opt}$.

Set $c^\epsilon(x) := U(x/\epsilon)\mathbb{1}_{x<0} + s_R^{opt}\mathbb{1}_{x>0}$; as in (i), we check that this function is a bounded-flux solution of (15) for every $\epsilon > 0$. Indeed, differentiating (22) in the weak sense and recalling the definition of φ_L we see that equation (15a) is satisfied pointwise for $x \neq 0$. The capillary pressures are connected at $\{x = 0\}$ because $(\widetilde{s}_L^\pi, s_R^{opt}) \in \mathcal{P}$; and the fluxes are connected at $\{x = 0\}$ because

$$(f_L(c) - \epsilon\partial_x c)|_{x=0^-} = f_L(s_L^{opt}) = f_R(s_R^{opt}) = (f_R(c) - \epsilon\partial_x c)|_{x=0^+}.$$

The limit of $s^\epsilon(\cdot)$ being $c(x) := s_L^{opt}\mathbb{1}_{x<0} + s_R^{opt}\mathbb{1}_{x>0}$, this ends the proof for this case.

In the second case, we have $\widetilde{s}_L^\pi = s_L^{opt}$, $s_R^{opt} < \widetilde{s}_R^\pi$, and $f_R(\cdot) - f_R(s_R^{opt}) \leq 0$ on $[0, 1]$. Analogously to the first case, we construct a profile $c^\epsilon(x) := s_L^{opt}\mathbb{1}_{x<0} + U(x/\epsilon)\mathbb{1}_{x>0}$. Here $U(\cdot)$ is a non-increasing function with $\lim_{\xi \to +\infty} U(\xi) = s_R^{opt}$; it solves the ODE problem analogous to (22) but posed on $[0, +\infty)$, with $f_R, \widetilde{s}_R^\pi, s_R^{opt}$ replacing $f_L, \widetilde{s}_L^\pi, s_L^{opt}$, respectively. □

With the above proposition in hand, we highlight the following

Selection Rule: *We set (s_L^π, s_R^π) to be the intersection point of $\mathcal{U}$ and $\mathcal{P}$ if the two curves cross (see Fig. 1), and we set it to be (s_L^{opt}, s_R^{opt}) if $\mathcal{U}$ and $\mathcal{P}$ do not cross.*

2 Buckley-Leverett equation in two-rocks' medium

Taking the limit $\epsilon \to 0$ in the problem (15) provides formally that the limit s of s^ϵ satisfies the hyperbolic scalar conservation law with discontinuous flux function

$$\phi(x)\partial_t s + \partial_x f(x, s) = 0, \tag{23}$$

that is known to have several mathematically consistent notions of solution (see [2]). In Section 2.1, we recall some elements of the theory on the scalar conservation laws with discontinuous flux functions detailed in [7], that will be of great interest to identify the notion of solution that describes the vanishing capillarity limit.

2.1 The formal discontinuous-flux model, connections, entropy solutions

Buckley-Leverett equation in two-rocks' medium is a particular case of conservation law with discontinuous flux. When the interface between the media is located at $\{x = 0\}$, this general problem takes the form

$$\partial_t\left[(\phi_L\mathbb{1}_{x<0} + \phi_R\mathbb{1}_{x>0})s\right] + \partial_x\left[f_L(s)\mathbb{1}_{x<0} + f_R(s)\mathbb{1}_{x>0}\right] = 0. \tag{24}$$

Remark 1 *In the case $\phi_L = \phi_R$, problem (24) has been much studied in the literature (see the references in [7]). Let us stress that the introduction of constant coefficients ϕ_L and ϕ_R does not change the properties of problem: namely, the definitions and results stated below can be reduced to those of [7] and the other references upon introducing the new unknown $u(x,t) := (\phi_L \mathbb{1}_{x<0} + \phi_R \mathbb{1}_{x>0}) s(x,t)$ and the new fluxes $g_{L,R} : u \mapsto f_{L,R}(u/\phi_{L,R})$.*

The notion of L^1-*dissipative germ* (L^1D germ, for short) has been formulated in [7] in order to describe the different semigroups of entropy solutions satisfying the L^1 contraction principle. For fluxes $f_{L,R}$ satisfying (**A1**), (24) can be seen as the formal limit, as $\epsilon \to 0$, of (15). We interpret this idea by saying that an admissible solution s to (24), in the Buckley-Leverett context, should be a *vanishing capillarity limit*, i.e., a limit of some sequence $(s^\epsilon)_{\epsilon \to 0}$ of solutions of (15). Due to Theorems 1,2, it is clear that the vanishing capillarity limits do satisfy the L^1 contraction principle; thus the setting of [7] is suitable for our needs.

Let us give the definitions underlying the theory of problem (24).

Definition 3 (admissibility germs; complete, maximal and definite germs)

· *Any set $\mathcal{G}$ of couples $(s_L, s_R) \in [0,1]^2$ satisfying the Rankine-Hugoniot relation*

$$\forall (s_L, s_R) \in \mathcal{G} \quad f_L(s_L) = f_R(s_R) \tag{25}$$

and the L^1-dissipativity relation

$$\forall (s_L, s_R), (z_L, z_R) \in \mathcal{G} \quad \Phi_L(s_L, z_L) \geq \Phi_R(s_R, z_R) \tag{26}$$

is called an L^1D admissibility germ (a germ, for short) associated with the couple of fluxes (f_L, f_R) defined on $[0,1]$.

· *A germ $\mathcal{G}$ is called complete if all Riemann problem at $x = 0$ for (24) admits a self-similar solution s such that $(s_L, s_R) \in \mathcal{G}$, where s_L, resp. s_R, is the limit of $s(t, \cdot)$ as $x \to 0^-$, resp. as $x \to 0^+$.*

· *We say that $\mathcal{G}'$ is an extension of a germ $\mathcal{G}$ if $\mathcal{G} \subset \mathcal{G}'$ and $\mathcal{G}'$ still satisfies the L^1-dissipativity property in (26) and the Rankine-Hugoniot condition in (25).*

· *A germ $\mathcal{G}$ is called maximal, if it does not admit a nontrivial extension.*

· *A germ $\mathcal{G}$ is called definite, it it admits only one maximal extension.*

In relation with definite and maximal germs, consider one more definition.

Definition 4 (dual of a germ) *Let $\mathcal{G}$ be an L^1D-admissibility germ. The dual of $\mathcal{G}$ is the set*

$$
\mathcal{G}^* := \Big\{ (z_L, z_R) \in [0,1]^2 \;\Big|\; f_L(z_L) = f_R(z_R) \\
\text{and for all } (s_L, s_R) \in \mathcal{G}, \; \Phi_L(s_L, z_L) \geq \Phi_R(s_R, z_R) \Big\}. \tag{27}
$$

It is shown in [7] that, if $\mathcal{G}$ is a definite germ, then its dual $\mathcal{G}^*$ is the unique maximal extension of $\mathcal{G}$.

We are in a position to define different notions of entropy solution. For simplicity, consider a finite time horizon $T > 0$.

Definition 5 *Given a couple of continuous functions (f_L, f_R) defined on $[0,1]$ and a definite germ $\mathcal{G}$ associated with this couple, we say that $s \in L^\infty(\mathbb{R} \times (0,T); [0,1])$ is a $\mathcal{G}$-entropy solution of (24) if the Kruzhkov entropy inequalities hold away from the interface $\{x = 0\}$:*

$$\forall \kappa \in [0,1] \quad \partial_t (\phi_{L,R} |s - \kappa|) - \partial_x \Phi_{L,R}(s, \kappa) \leq 0 \quad \text{in} \quad \mathcal{D}'(\Omega_{L,R} \times (0,T)), \tag{28}$$

and and for a.e. $t \in (0,T)$, one has $(s_L(t), s_R(t)) \in \mathcal{G}^*$, where $s_L(\cdot)$ (the trace as $x \to 0^-$) and $s_R(\cdot)$ (the trace as $x \to 0^+$) are the interface traces of s in the strong $L^1(0,T)$ sense.

We say that s is a $\mathcal{G}$-entropy solution of the Cauchy problem with $s(\cdot, 0) = s_0$ if the initial condition s_0 is assumed in the sense of strong L^1_{loc} initial trace.

Notice that under assumption (**A1**), the traces $s_{L,R}$ and $s(\cdot, 0)$ do exist ([51, 44, 45, 27]).

Remark 2 *According to the results of [51], [44] and [27], it is not a restriction to assume that, up to a re-definition of $u(t, \cdot)$ on a set of zero measure of $t \in [0, T]$, a $\mathcal{G}$-entropy solution of (24) belongs to $C([0, T]; L^1_{loc}(\mathbb{R}))$.*

The following result is contained in [7] (see in particular [7, Theorem 6.4])

Theorem 3 (Well-posedness for $\mathcal{G}$-entropy solutions) *Assume (**A1**) holds, and $\mathcal{G}$ is a definite germ of which the dual $\mathcal{G}^*$ is complete. Then for all measurable initial datum s_0 with values in $[0, 1]$ there exists a unique $\mathcal{G}$-entropy solution to problem (24). Moreover, the finite volume scheme for (24) with Godunov flux converges to the corresponding $\mathcal{G}$-entropy solution, for all initial datum.*

Remark 3 *It is required in [7, Theorem 6.4] that $f_{L,R}$ be defined on $\mathbb{R}$. Let us point out that in our case, solutions with $[0, 1]$-valued initial data always take values in $[0, 1]$. Indeed, assumptions (**A1**) contain the compatibility conditions $f_L(0) = f_R(0)$, $f_L(1) = f_R(1)$. Moreover, it is easily seen that $(0, 0)$ and $(1, 1)$ belong to $\mathcal{G}^*$, whatever be the germ $\mathcal{G}$; therefore 0 and 1 are constant $\mathcal{G}$-entropy solutions. This ensures, in particular, that approximate solutions constructed by the Godunov scheme lie in between zero and one.*

Under assumptions (**A1**), it is easy to classify all possible L^1D admissibility germs. According to the analysis of [7, Section 4.8][1], each maximal germ is complete, and it is entirely determined by a definite germ which is a singleton. Such singletons are called *connections* in the below definition.

Definition 6 (Adimurthi et al. [2], Bürger et al. [20]) *For $f_{L,R}$ satisfying (**A1**), a couple $(A, B) \in [0, 1]^2$ is said to be a* connection *if $A \in [\bar{s}_L, 1]$, $B \in [0, \bar{s}_R]$ and $f_L(A) = f_R(B)$.*

Being a connection means that $u(t, x) := A\mathbb{1}_{x<0} + B\mathbb{1}_{x>0}$ is a stationary weak solution of (24) that represents an undercompressive shock: the (strict) Lax condition fails from *both* sides from the jump.

Notice that the set $\mathcal{U}$ of all connections (see Fig. 1) is given by (21). Let us describe its extremities. We define the *optimal connection* (A^{opt}, B^{opt}) by

$$(A^{opt}, B^{opt}) \in \mathcal{U}, \text{ with either } A^{opt} = \bar{s}_L \text{ or } B^{opt} = \bar{s}_R.$$

and the *barrier connection* (A^{bar}, B^{bar}) by

$$(A^{bar}, B^{bar}) \in \mathcal{U}, \text{ with either } A^{bar} = 1 \text{ or } B^{bar} = 0.$$

The common value $\bar{F} = f_L(A) = f_R(B)$ is called the *connection level* and denoted by $\bar{F}_{(A,B)}$; when (A, B) runs over $\mathcal{U}$, $\bar{F}_{(A,B)}$ fills the interval $[\bar{F}^{bar}, \bar{F}^{opt}]$; here $\bar{F}^{bar} = \max\{0, q\} = f_L(A^{bar}) = f_R(B^{bar})$, while $\bar{F}^{opt} = \min\{\max_{[0,1]} f_L, \max_{[0,1]} f_R\} = f_L(A^{opt}) = f_R(B^{opt})$.

Reciprocally, the connection at level $\bar{F} \in [\bar{F}^{bar}, \bar{F}^{opt}]$ is denoted by $(A_{\bar{F}}, B_{\bar{F}})$. Such a connection is indeed unique, since $f_{L,R}$ are strictly monotone on $[0, \bar{s}_{L,R}]$ and on $[\bar{s}_{L,R}, 1]$.

Further, set $\mathcal{O} := \mathcal{G}^*_{(A^{opt}, B^{opt})}$ (see Fig.2b). From the bell-shapedness assumption in (**A1**) one easily sees that $\mathcal{O} \setminus \{(A^{opt}, B^{opt})\}$ is the set of all couples $(a, b) \in [0, 1]^2 \setminus \mathcal{U}$ such that $f_L(a) = f_R(b)$. In contrast to *under-compressive states* $(A, B) \in \mathcal{U}$, every couple $(a, b) \in \mathcal{O}$ will be called an *over-compressive state* (note that $(A^{opt}, B^{opt}) \in \mathcal{U} \cap \mathcal{O}$ is both under- and over-compressive). We have

Proposition 4 (see Section 4.8 in [7], see also [4])
For every connection $(A, B) \in \mathcal{U}$, the singleton $\mathcal{G}_{(A,B)} := \{(A, B)\}$ is a definite germ; its dual is given by

$$\mathcal{G}^*_{(A,B)} = \{(A, B)\} \cup \mathcal{O}_{\bar{F}_{(A,B)}}, \text{ where } \mathcal{O}_{\bar{F}_{(A,B)}} := \left\{ (z_L, z_R) \in \mathcal{O} \text{ s.t. } f_L(z_L) = f_R(z_R) \leq \bar{F}_{(A,B)} \right\}. \quad (29)$$

Moreover, every maximal germ contains one and only one connection $(A, B) \in \mathcal{U}$, therefore it can be represented under the form (29).

Remark 4 *The point of view developed in our note [4] is that, at least for the purpose of interpretation of the solutions' behavior and for their numerical approximation, it is convenient to characterize different notions of $\mathcal{G}$-entropy solution by the connection level $\bar{F}$ rather than by the corresponding connection $(A_{\bar{F}}, B_{\bar{F}})$. Indeed, as one can see from the representation (29), the possible trace couples (s_L, s_R) of $\mathcal{G}_{(A_{\bar{F}}, B_{\bar{F}})}$-entropy solutions obey the constraint $f_{L,R}(s_{L,R}) \leq \bar{F}$. In particular, the only free parameter required to construct the Godunov scheme for problem (24) with fluxes (**A1**) is the connection level $\bar{F}$ (see [4] and Section 3.2 below for details).*

---

[1]While this analysis has been carried out under the assumption $q = 0$, the general case is completely analogous
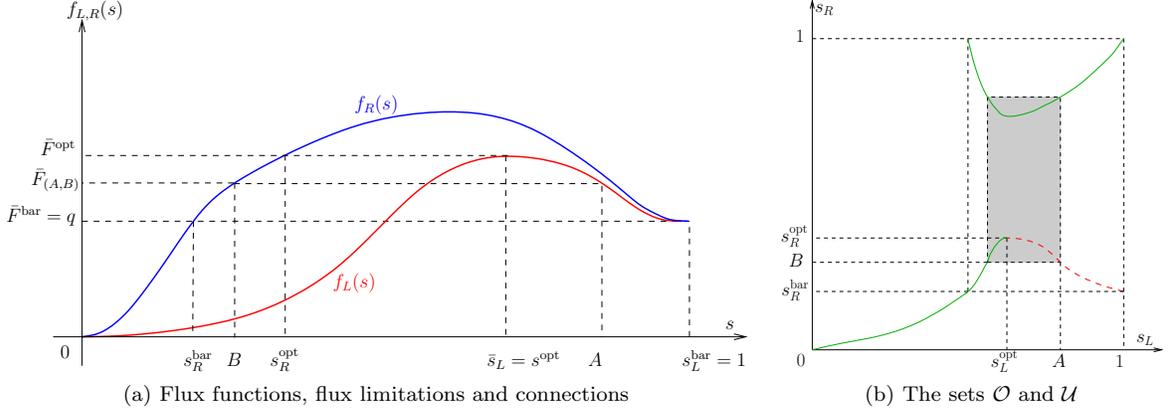
(a) Flux functions, flux limitations and connections   (b) The sets $\mathcal{O}$ and $\mathcal{U}$

Figure 2: On Figure 2a, the two flux functions $f_{L,R}$ have been plotted. Given a value $\bar{F}_{(A,B)} \in [\bar{F}^{\mathrm{bar}}, \bar{F}^{\mathrm{opt}}]$, we construct the unique corresponding connection $(A,B) \in \mathcal{U}$. On Figure 2b, we have plotted the corresponding sets $\mathcal{O}$ (green solid line) and $\mathcal{U}$ (red dashed line). For a given flux limitation $\bar{F}_{(A,B)}$, the grey rectangle represents the open set $\{(s_L, s_R) \in [0,1]^2 \mid (f_L(s_L) > \bar{F}_{(A,B)}) \& (f_R(s_R) > \bar{F}_{(A,B)})\}$. So, the maximal germ $\mathcal{G}^*_{(A,B)}$ is made of the union of singleton $\{(A,B)\}$ and of the subset $\mathcal{O}_{\bar{F}_{(A,B)}}$ of $\mathcal{O}$ which is outside of the grey rectangle.

Finally, we recall an equivalent characterization of $\mathcal{G}_{(A,B)}$-entropy solutions with the help of *adapted entropy inequalities* introduced by Baiti and Jenssen [11] and Audusse and Perthame [8].

Theorem 4 (see [7], see also [20]) *Given a connection $(A,B) \in \mathcal{U}$, a function $s \in L^\infty(\mathbb{R} \times (0,T))$ is a $\mathcal{G}_{(A,B)}$-entropy solution of* (24) *with fluxes (A1) if and only if it satisfies, away from the interface, the Kruzhkov entropy inequalities* (28) *and moreover, given $c(x) = A\mathbb{1}_{x<0} + B\mathbb{1}_{x>0}$, it satisfies the global adapted entropy inequality*

$$\partial_t\big(\phi(x)|s - c(x)|\big) - \partial_x\Phi(x;s,c(x)) \leq 0 \quad in \quad \mathcal{D}'(\mathbb{R} \times (0,T)). \tag{30}$$

Here $\phi(x) = \phi_L\mathbb{1}_{x<0} + \phi_R\mathbb{1}_{x>0}$; similarly, $\Phi(x;s,c) = \Phi_L(s,c)\mathbb{1}_{x<0} + \Phi_R(s,c)\mathbb{1}_{x>0}$.

2.2 Identifying the vanishing capillarity solutions

Combining the results of the previous sections, we can state and prove our main result.

Theorem 5 (Main result) *Assume we are given nonlinearities $f_{L,R}$ and $\pi_{L,R}$ satisfying (A1),(A2),(A3).*

Let $(s_L^\pi, s_R^\pi) \in \mathcal{U}$ be the connection obtained according to the Selection Rule *of Section 1.3, i.e., it is either the intersection point of the curves $\mathcal{U}$ and $\mathcal{P}$ (see Fig.1) or the optimal connection (s_L^{opt}, s_R^{opt}) when $\mathcal{U} \cap \mathcal{P} = \emptyset$.*

Then s is a $\mathcal{G}_{(s_L^\pi, s_R^\pi)}$-entropy solution of the discontinuous-flux Buckley-Leverett equation (24) *if and only if s can be obtained at the a.e. limit of solutions s^ϵ of* (15) *as the capillarity parameter ϵ vanishes.*

In particular, any solution of (24) *obtained as vanishing capillarity limit obeys the flux limitation constraint at the interface: $f_L(s(t,0^-)) = f_R(s(t,0^+)) \leq \bar{F}^\pi$ where $\bar{F}^\pi = f_{L,R}(s_{L,R}^\pi)$ is the corresponding connection level.*

Proof: Fix some (not labelled) sequence ϵ decreasing to zero. According to Theorem 2, problem (15) is well posed in the setting of mild solutions, moreover, the Kato inequality holds for all couple of solutions. Assume for a moment that

given s^ϵ corresponding to a given datum s_0, one can extract an L^1_{loc}-convergent subsequence $s^\epsilon \to s$. (31)

First, write the Kato inequality (17) for a solution s^ϵ and for the capillarity profile c^ϵ constructed in Proposition 3. Using the convergence $s^\epsilon \to s$, $c^\epsilon \to c$ as $\epsilon \to 0$, $c(x) = c_L^\pi\mathbb{1}_{x<0} + c_R^\pi\mathbb{1}_{x>0}$, we can pass to the limit in this inequality. We inherit the "hyperbolic Kato inequality"

$$\sum_{i \in \{L,R\}} \iint_{\Omega_i \times \mathbb{R}_+} \Big(\phi_i|s - c(x)|\partial_t\psi + \Phi_i(s,c(x))\partial_x\psi\Big) + \sum_{i \in \{L,R\}} \int_{\Omega_i} \phi_i|s_0 - c(x)|\psi(\cdot,0) \geq 0$$

11

for all $\psi \in \mathcal{D}(\mathbb{R} \times [0,T))$, $\psi \geq 0$. Restricting the choice of test functions to $\mathcal{D}(\mathbb{R} \times (0,T))$, we find the global adapted entropy inequality (30) with $(A,B) = (s_L^\pi, s_R^\pi)$. Second, with the classical arguments one readily sees that s is a Kruzhkov entropy solution away from the interface, in the sense (28); moreover, it assumes the initial datum s_0. Therefore, s is the (unique) $\mathcal{G}_{(s_L^\pi, s_R^\pi)}$-entropy solution with datum s_0. Thus, provided (31) is justified, we prove that every $\mathcal{G}_{(s_L^\pi, s_R^\pi)}$-entropy solution is a vanishing viscosity limit.

Reciprocally, assume s is the a.e. limit of some sequence $(s^\epsilon)_\epsilon$ of solutions of (15) corresponding to initial data $(s_0^\epsilon)_\epsilon$. Since all solutions are $[0,1]$-valued, we also have the $L^1_{loc}(\mathbb{R} \times [0,T])$ convergence of s^ϵ to s. As above, we see that s is an entropy solution of (24) away from the interface, and s verifies the adapted entropy inequality (30) with $(A,B) = (s_L^\pi, s_R^\pi)$. Therefore, it is a $\mathcal{G}_{(s_L^\pi, s_R^\pi)}$-entropy solution. This ends the proof of the theorem, except for the justification of (31).

If we assume that $f_{L,R}$ are genuinely nonlinear on every interval, then according to the well-known compactification results of [41, 43, 46] we can extract an L^1_{loc} convergent subsequence of s^ϵ. In the general case, we can use the framework of $\mathcal{G}$-entropy-process solutions in the way of [5]. Indeed, extracting a nonlinear weakly-$*$ convergent subsequence of $(s^\epsilon)_\epsilon$, due to the existence of $\mathcal{G}$-entropy solutions (see Theorem 3) we can prove that the $\mathcal{G}_{(s_L^\pi, s_R^\pi)}$-entropy-process solution coincides with the unique $\mathcal{G}_{(s_L^\pi, s_R^\pi)}$-entropy solution for the same initial datum. Let us point out that the proof is not straightforward, because one global adapted entropy inequality (as in Theorem 4) is not sufficient in this argument (see [5] for the case $f_L \equiv f_R$). $\qquad\square$

Remark 5 *Another way to prove* (31) *is to restrict our attention to a dense set of initial data s_0, and to derive additional estimates on the solution, like a BV estimate on a Temple function [10, 31, 24], or, using a variant of the technique of Bürger, García, Karlsen and Towers [18, 20], one can derive a BV_{loc} estimate on the solution with small capillarity s^ϵ. This latter point is detailed in Appendix A.1.*

3   Numerical approximation of the flow in two-rocks' medium

The goal of this section is, first of all, to provide numerical evidence for convergence of s^ϵ towards the appropriate entropy solution s (recall that the notion of solution strongly depends on the capillarity profiles $\pi_{L,R}$, see Section 2, and secondly, to discuss about "time saved versus accuracy lost" by solving the simpler problem (24) instead of solving the finer problem (15). To do so, we introduce two numerical schemes: the first one, used to discretize the parabolic problem (15), was proved to be convergent by the second author in [23]; the second one, introduced by the authors in [4], is the exact Godunov scheme adapted to the connection (s_L^π, s_R^π), and is based on the notion of flux limitation ([31]) discussed in Section 2.1.

3.1   A finite volume scheme for the parabolic model

First, we have to compute the mild solutions s^ϵ of the degenerate parabolic problem (15). This is done by means of the fully implicit finite volume scheme studied in [34, 23].

For $\Delta x > 0$, we denote by $\left(x_{j+1/2}\right)_{j \in \mathbb{Z}} = \{(j+1/2)\Delta x \mid j \in \mathbb{Z}\}$ the set of the "cell centers" and by $(x_j)_{j \in \mathbb{Z}} = \{j\Delta x \mid j \in \mathbb{Z}\}$ the sets of the "edges". Given $\Delta t > 0$, we use $(t^n)_n = \{n\Delta t \mid n \in \mathbb{N}\}$ for time steps.

For $s_0 \in L^\infty(\mathbb{R}; [0,1])$, the initial data is discretized as follows:

$$s_{j+1/2}^{\epsilon,0} = \frac{1}{\Delta x} \int_{x_j}^{x_{j+1}} s_0(x)\mathrm{d}x. \tag{32}$$

The implicit scheme is then given by

$$\forall j \in \mathbb{Z}, \forall n \in \mathbb{N}, \qquad \phi_j \frac{s_{j+1/2}^{\epsilon,n+1} - s_{j+1/2}^{\epsilon,n}}{\Delta t}\Delta x + F_{j+1}^{\epsilon,n+1} - F_j^{\epsilon,n+1} = 0, \tag{33}$$

where the fluxes $F_j^{\epsilon,n+1}$ have to be made explicit. Let $j \in \mathbb{Z} \setminus \{0\}$; for ψ standing for one of the symbols $\phi, f, \varphi, \pi, \overline{s}$, we denote a space dependent function which is constant in $\Omega_{L,R}$ as follows:

$$\psi_j := \psi(\cdot, x_j) = \left\{ \begin{array}{ll} \psi_L & \text{if } j < 0 \\ \psi_R & \text{if } j > 0. \end{array} \right.$$

We introduce now the exact Riemann solver for the convection within $\Omega_{L,R}$. For $(a,b) \in [0,1]^2$ and $j \in \mathbb{Z} \setminus \{0\}$, we set

$$G_j(a,b) = \left\{ \begin{array}{ll} \min_{s \in [a,b]} f_j(s) & \text{if } a \leq b, \\ \min_{s \in [a,b]} f_j(s) & \text{if } a \geq b. \end{array} \right.$$

Note that $G_j(a,a) = f_j(a)$, that G_j is Lipschitz continuous w.r.t. both variables, and that G_j is non-decreasing w.r.t to its first argument and non-increasing w.r.t. the second. It is well known that for bell-shaped fluxes, G_j can be computed by the formula

$$G_j(a,b) = \min\left(f_j(\min(a, \overline{s}_j)), f_j(\max(b, \overline{s}_j))\right); \tag{34}$$

let us recall that $\overline{s}_{L,R} = \arg\max f_{L,R}$ (see Assumption **(A1)**).

For $j \neq 0$ (i.e. in the case where the edge j is not at the interface), one defines

$$F_j^{\epsilon,n+1} = G_j(s_{j-1/2}^{\epsilon,n+1}, s_{j+1/2}^{\epsilon,n+1}) - \epsilon \frac{\varphi_j(s_{j+1/2}^{\epsilon,n+1}) - \varphi_j(s_{j-1/2}^{\epsilon,n+1})}{\Delta x}. \tag{35}$$

It remains to define the flux $F_0^{\epsilon,n+1}$ across the interface so that everything be defined in (33). To do so, following [34], we introduce additional unknowns $s_{0,L}^{\epsilon,n+1}, s_{0,R}^{\epsilon,n+1}$ that solve the following nonlinear system

$$\tilde{\pi}_L(s_{0,L}^{\epsilon,n+1}) \cap \tilde{\pi}_R(s_{0,R}^{\epsilon,n+1}) \neq \emptyset, \tag{36a}$$

$$F_0^{\epsilon,n+1} := G_L(s_{-1/2}^{\epsilon,n+1}, s_{0,L}^{\epsilon,n+1}) - \epsilon \frac{\varphi_L(s_{0,L}^{\epsilon,n+1}) - \varphi_L(s_{-1/2}^{\epsilon,n+1})}{\Delta x/2} \tag{36b}$$

$$= G_R(s_{0,R}^{\epsilon,n+1}, s_{1/2}^{\epsilon,n+1}) - \epsilon \frac{\varphi_R(s_{1/2}^{\epsilon,n+1}) - \varphi_L(s_{0,R}^{\epsilon,n+1})}{\Delta x/2}. \tag{36c}$$

It is proven in [23] that for all $(s_{-1/2}^{\epsilon,n+1}, s_{1/2}^{\epsilon,n+1})$, the system (36) admits a unique solution $(s_{0,L}^{\epsilon,n+1}, s_{0,R}^{\epsilon,n+1})$, hence the flux $F_0^{\epsilon,n+1}$ is well defined.

The results of the paper [23] can be summarized as follows.

Proposition 5 *Let $\epsilon > 0$ be fixed and let $s_0 \in L^\infty(\mathbb{R}; [0,1])$, then*

1. *the scheme (33),(35),(36) admits a unique solution $\left(s_{j+1/2}^{\epsilon,n+1}\right)_{j \in \mathbb{Z}, n \in \mathbb{N}}$;*

2. *if we define the approximate solution s_h^ϵ almost everywhere on $\mathbb{R}_+ \times \mathbb{R}$ by*

$$s_h^\epsilon(x,t) = s_{j+1/2}^{\epsilon,n+1} \quad \text{if } (x,t) \in (x_j, x_{j+1}) \times (t^n, t^{n+1}),$$

then $s_h^\epsilon \in L^\infty(\mathbb{R} \times \mathbb{R}_+; [0,1])$ converges in $L^1_{\text{loc}}(\mathbb{R} \times \mathbb{R}_+)$ towards the unique mild solution of the problem as $\Delta x, \Delta t \to 0$.

3.2 A finite volume scheme for the hyperbolic model

The scheme introduced in previous section is *asymptotic preserving*, in the sense that choosing $\epsilon = 0$, and obtaining therefore an approximate solution s_h^0 (the solution to the scheme in the case $\epsilon = 0$ is once again unique), one can show that s_h^0 tends to the vanishing capillarity limit described in Theorem 5. This point is made explicit in Appendix A.2. Nevertheless, to produce numerical results for the hyperbolic problem (24), we use the Godunov scheme under the form explained in our note [4] (see also [30]). Namely, we have shown in [4, Theorem 3.1] that in order to obtain the Godunov scheme for approximation of $\mathcal{G}_{(A,B)}$-entropy solutions of (24) with fluxes **(A1)**, it is enough to take the scheme of Adimurthi et al. [1] known for the optimal connection (A^{opt}, B^{opt}) and to limit the flux at the interface to the maximum value $\overline{F}_{(A,B)}$. More precisely, in our case, the *explicit* Godunov scheme for computing the unique $\mathcal{G}_{(s_L^\pi, s_R^\pi)}$-entropy solution can be rewritten as

$$\phi_j \frac{s_{j+1/2}^{n+1} - s_{j+1/2}^n}{\Delta t} \Delta x + F_{j+1}^n - F_j^n = 0, \tag{37}$$

where the fluxes F_j^n are given by

$$F_j^n = G_j(s_{j-1/2}^n, s_{j+1/2}^n) \quad \text{if } j \neq 0, \tag{38}$$

$$F_0^n = \min\left(\overline{F}^\pi, f_L(\min(s_{-1/2}^n, \overline{s}_L)), f_R(\max(s_{1/2}^n, \overline{s}_L))\right). \tag{39}$$

13

In the previous formula (38), the exact Riemann solver G_j was defined by (34) while, in formula (39), the quantity $\bar{F}^\pi = f_{L,R}(s_{L,R}^\pi)$ is the connection level corresponding to the connection chosen using the selection rule of Section 1.3.

We now state a convergence result which is a consequence of the fact that the scheme prescribed by (37)–(39) is monotone and preserves $\mathcal{G}_{(s_L^\pi, s_R^\pi)}$ (it even preserves $\mathcal{G}_{(s_L^\pi, s_R^\pi)}^*$ since the scheme is the Godunov one). Recall that it has been stated in Theorem 3 that the Godunov scheme is convergent. We refer to [7, 4] for further explanations.

Proposition 6 *Define $s_h : \mathbb{R} \times \mathbb{R}_+ \to \mathbb{R}$ by $s_h(x,t) = s_{j+1/2}^{n+1}$ if $(x,t) \in (x_j, x_{j+1}) \times (t^n, t^{n+1})$, then, if we denote by $\mathcal{L}_f$ a Lispchitz constant of both $f_{L,R}$, and if there exists $\zeta \in (0,1)$ such that*

$$\Delta t \leq \frac{(1-\zeta)\Delta x}{\mathcal{L}_f}, \tag{40}$$

then $s_h \in L^\infty(\mathbb{R} \times \mathbb{R}_+; [0,1])$. Moreover, under the CFL condition (40), when Δx (and thus also Δt) tends to zero the discrete solution s_h converges in $L_{\mathrm{loc}}^1(\mathbb{R} \times \mathbb{R}_+)$ towards the unique $\mathcal{G}_{(s_L^\pi, s_R^\pi)}$-entropy solution of the problem.

3.3 Numerical illustrations of convergence

We now give numerical evidence of convergence of the mild solution s^ϵ of the parabolic problem towards the $\mathcal{G}_{(s_L^\pi, s_R^\pi)}$-entropy solution by comparing their respective approximations s_h^ϵ and s_h.

3.3.1 The test cases

Concerning the design of the test cases, we have chosen a particularly simple configuration. The capillary pressure functions $\pi_{L,R}$ are defined by

$$\pi_{L,R}(s) = P_{L,R} - \ln(1-s), \tag{41}$$

where the quantities $P_{L,R}$, called *entry pressures*, play an important role in the selection of the correct solution notion (cf. Section 1.3) and will vary from one case to another. Note that in the case where $P_R \geq P_L$, the
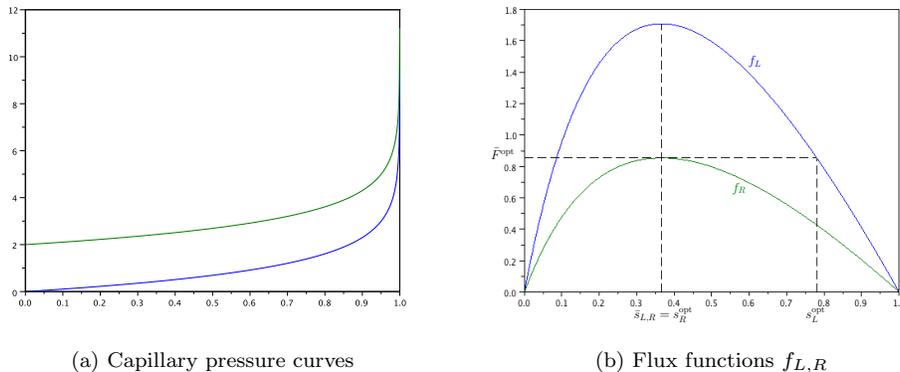

(a) Capillary pressure curves

(b) Flux functions $f_{L,R}$

Figure 3: The capillary pressure curves (Fig. 3a) defined by (41)—here $P_L = 0$ (blue) and $P_R = 2$ (green)— satisfy $\lim_{s\to 1} \pi_{L,R}(s) = +\infty$. Therefore, the maximal extension $\tilde{\pi}_{L,R}$ of $\pi_{L,R}$ is obtained by adding $\{0\} \times [-\infty, P_{L,R})$ and $\{1\} \times \{+\infty\}$ to the graph $\{(s, \pi_{L,R}(s) \mid s \in [0,1)\}$. For the particularly simple choice of parameters and functions done in the simulations, the flux functions $f_{L,R}$ are proportional one to the other. We have represented on Fig. 3b the optimal connection that is relevant for the case presented in Section 3.3.2, but not in the one presented in Section 3.3.3.

set $\mathcal{P}$ defined in Section 1.3 by (20) has the particular simple expression

$$\mathcal{P} = \left\{ \left(s, \max\left\{ 0, 1 + (s-1)e^{P_R - P_L} \right\} \right), \ s \in [0,1] \right\}.$$
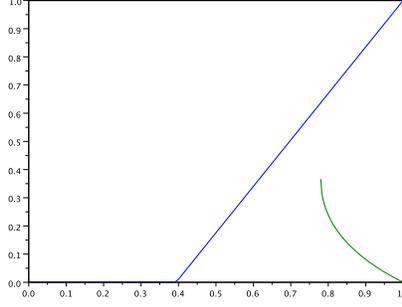
Figure 4: The connection diagram in a case where the intersection of $\mathcal{P}$ (in blue) and $\mathcal{U}$ (in green) is empty; according to the Selection Rule of Section 1.3, it leads to considering the optimal entropy solution.

Numerical values of the parameters. The only parameter we let vary between the two test cases is the entry pressure P_R. In the first case, which leads to the optimal connection, we choose $P_R = 0.5$. In the second case, we chose $P_R = 2$, so that the selection rule presented in Section 1.3 provides another solution, despite the fact that formally, the equation remains the same. The physical parameters and functions used in the simulations are collected in the following tables. Concerning the scaling parameter ϵ, several values has been used in order to illustrate the convergence of s^ϵ towards s (see Fig. 10). All the numerical tests have been performed for the initial data $u_0 \equiv 0.5$.

| total flow rate	$q = 0$;	viscosities	$\mu_a = 10^{-3}$,
gravity	$g = -9.81$;		$\mu_b = 3.10^{-3}$;
intrinsic permeabilities	$K_L = 10^{-2}$, $K_R = 5.10^{-3}$;	densities	$\rho_a = 0.87$,
porosity	$\phi_L = \phi_R = 1$;		$\rho_b = 1$;
entry pressures	$P_L = 0$,	relative permeabilities	$kr_{a,i}(s) = s$,
	$P_R = 0.5$ in Section 3.3.2,		$kr_{b,i}(s) = (1-s)$;
	$P_R = 2$ in Section 3.3.3;	time step	$\Delta t = 2.5 * 10^{-3}$,
		space step	$\Delta x = 10^{-2}$.

3.3.2 The optimal connection

In the case where $P_R = 0.5$, the connection diagram (Fig. 4) is such that $\mathcal{P} \cap \mathcal{U} = \emptyset$. Therefore, the selection rule of Section 1.3 and Theorem 5 claim that the good notion of solution for the vanishing capillarity limit is the $\mathcal{G}_{(s_L^{\text{opt}}, s_R^{\text{opt}})}$-entropy solution.

The numerical approximation of the optimal entropy solution obtained via the Godunov scheme described in Section 3.2 is presented in Fig. 5a. It appears to be in good accordance with the solution for a small value of ϵ given by the implicit scheme described in Section 3.1, and represented on Fig. 5b. In particular, the wave starting from the interface with negative speed has the expected amplitude and the expected speed. As already noticed on Fig. 5, we see on Fig. 6 that the shocks of the hyperbolic solution are smoothed by adding some capillary diffusion. Let us also point out that the one-sided traces s_L, s_R of the hyperbolic solution on the interface $\{x = 0\}$ do not satisfy $\tilde{\pi}_L(s_L) \cap \tilde{\pi}_R(s_R) \neq \emptyset$. Therefore, these traces are not suitable for the parabolic approximation. We can see on both figures (particularly on Fig. 6a) that a boundary layer is present on the right hand side from the interface.

3.3.3 Another connection

Choosing now $P_R = 2$ provides the connection diagram presented in Fig. 7a, where it clearly appears that $\mathcal{P} \cap \mathcal{U} \neq \emptyset$. As previously, we denote by (s_L^π, s_R^π) the connection belonging to $\mathcal{P} \cap \mathcal{U}$. Following the selection rule of Section 1.3 and Theorem 5, the appropriate notion of entropy solution for the vanishing capillarity limit is then the $\mathcal{G}_{(s_L^\pi, s_R^\pi)}$-entropy solution. As a consequence, the interface flux is limited to the maximal value $\bar{F}^\pi$ (formally, the limitation is equal to $\bar{F}^{\text{opt}}$ in the case where the optimal entropy solution is selected).

Here again, the approximate solution s_h^ϵ for small capillarity ($\epsilon = 10^{-3}$) is really close to the vanishing capillarity solution (the $\mathcal{G}_{(s_L^\pi, s_R^\pi)}$-entropy solution). On Fig. 8, one can see that the shocks (for the hyperbolic
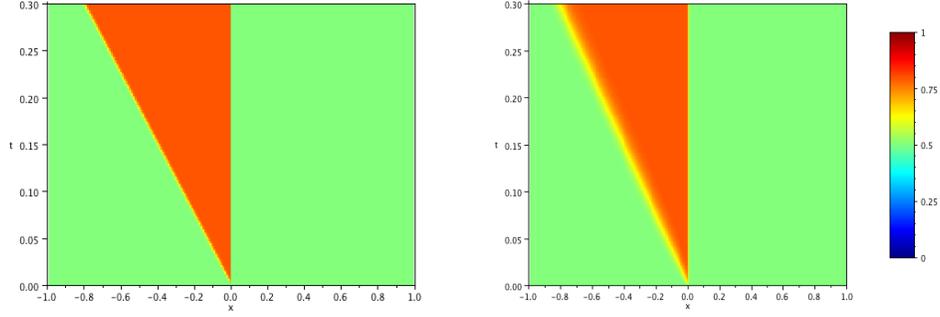
(a) Solution s_h to the hyperbolic problem   (b) Solution s_h^ϵ to the parabolic problem ($\epsilon = 10^{-3}$)

Figure 5
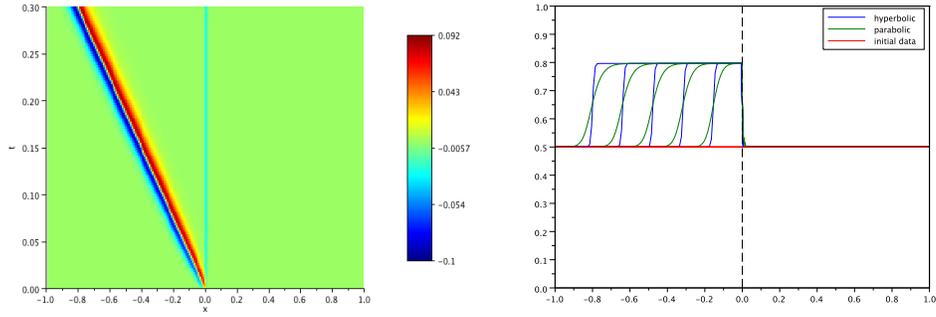
(a) Difference between s_h and s_h^ϵ (b) Solutions s_h and s_h^ϵ at different times

Figure 6
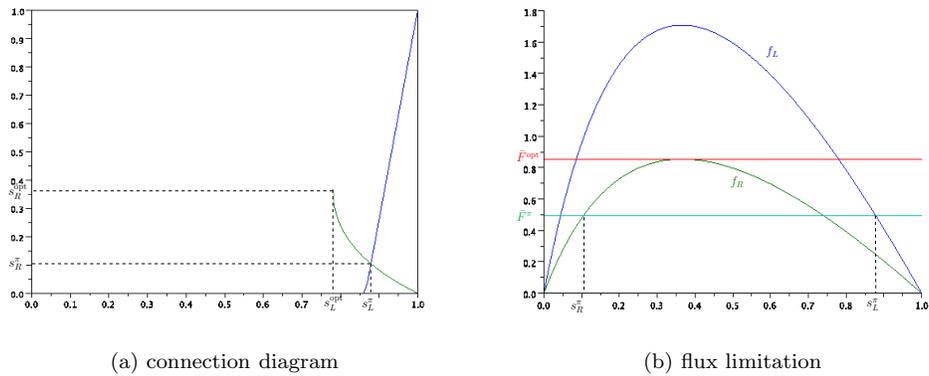
(a) connection diagram   (b) flux limitation

Figure 7: The connection diagram in a case where the intersection of $\mathcal{P}$ (in blue) and $\mathcal{U}$ (in green) is non-empty is presented on Fig. (7a). This results in a flux limitation, in the sense that at the interface, the flux of the hyperbolic solution may not exceed the value $\bar{F}^\pi = f_{L,R}(s_{L,R}^\pi)$, where (s_L^π, s_R^π) is the intersection point of $\mathcal{U}$ and $\mathcal{P}$.

16

solution) are smoothed in presence of capillary diffusion. Three waves are generated by the medium discontinuity: one wave with negative speed joining $s_0 = 0.5$ to $s_L^\pi \simeq 0.87$, one wave with zero speed joining s_L^π to $s_R^\pi \simeq 0.11$, and one wave with positive speed joining s_R^π to $s_0 = 0.5$. Note that since $\tilde{\pi}_L(s_L^\pi) \cap \tilde{\pi}_R(s_R^\pi) \neq \emptyset$, then there is no boundary layer for s^ϵ as $x \to 0$.

(a) Solution s_h to the hyperbolic problem   (b) Solution s_h^ϵ to the parabolic problem ($\epsilon = 10^{-3}$)
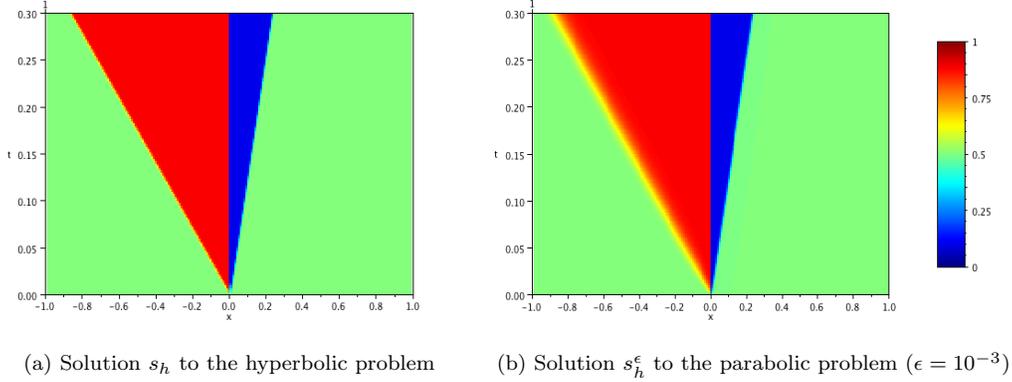
Figure 8

3.3.4 Convergence speed, numerical speed-up

One of the most important drawbacks of the numerical scheme presented in Section 3.1 for approximation of solutions to the parabolic problem is being implicit: the scheme requires the use of an iterative method at each time step, making the solution expensive to compute. For example, computing the approximate solution s_h^ϵ presented on Fig. 5b requires 2182.31 s of CPU time with Scilab, while the computation of the approximate solution s_h presented on Fig. 5a only requires 3.185 s of CPU time, the speed-up ration being hence of about 685. Moreover, since it is explicit, the computation of s_h requires less memory than the one needed to obtain s_h^ϵ; this allows to solve the hyperbolic problem on a finer mesh.

Concerning the convergence speed, we first illustrate in Fig. 10 the convergence of s^ϵ towards s by plotting $\log \|s_h^\epsilon - s_h\|_{L^1(0,T;L^1(-1,1))}$ as a function of ϵ. In accordance with the theory (see e.g. [15, 48]), Fig. 10 lets us think that for all $T > 0$, one has

$$\int_0^T \int_{\mathbb{R}} |s^\epsilon(x,t) - s(x,t)| \mathrm{d}x \mathrm{d}t \leq C\epsilon^{1/2}. \tag{42}$$

(a) Difference between both   (b) Plot of both solutions for different time t
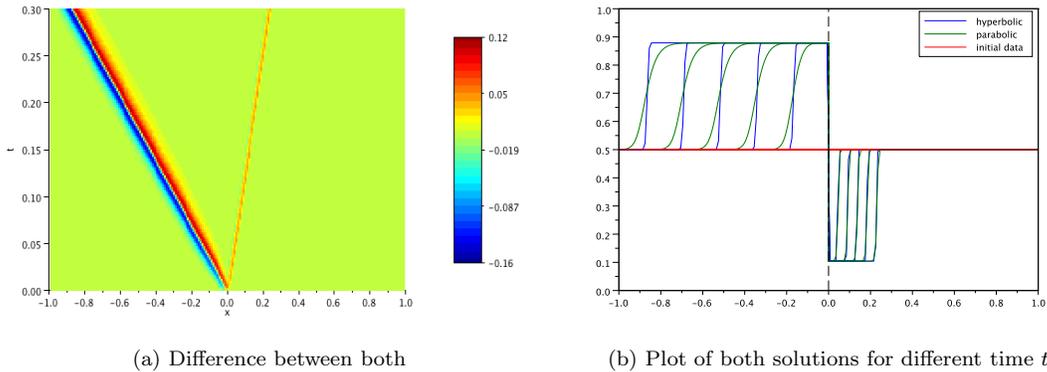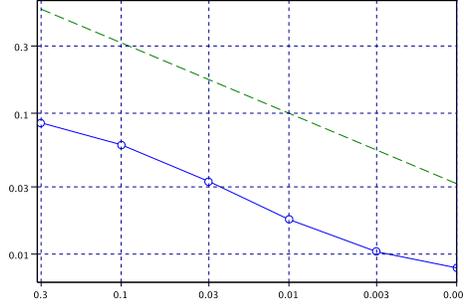
Figure 9

Figure 10: $\log \|s_h^\epsilon - s_h\|_{L^1(0,T;L^1(-1,1))}$ as a function of ϵ (in blue) and a straight line with slope $-1/2$ (dashed green). We recover numerically the order of convergence that was expected from (42). Note that the slope of the blue curve is damaged when ϵ is too large. This phenomenon is due to the fact that the solution is computed on the finite domain $x \in (-1,1)$. When the diffusion is large, the boundary conditions affects the numerical solution. The convergence rate is also damaged for small ϵ. This comes from the fact that the numerical error become comparable to the modeling error $\|s^\epsilon - s\|$ (this effect is particularly visible since the convection is discretized in an implicit way in the scheme presented in Section 3.1 and in an explicit way in the Godunov scheme presented in Section 3.2.

We now look at the convergence rate of the Godunov scheme. To our knowledge, no uniform bound on the total variation of s_h has been proved in the case $f_L \neq f_R$ (see [30] for the case $f_L \equiv f_R$). Yet the particularly simple configuration we are dealing with (a Riemann problem) ensures the existence of a variation bound. Carrying out a proof similar to the one performed in [30] provides an error estimate of type

$$\int_0^T \int_{\mathbb{R}} |s_h(x,t) - s(x,t)| \mathrm{d}x \mathrm{d}t \leq C \Delta x^{1/2}$$

(recall that $\Delta t \leq C \Delta x$ thanks to (40)) This estimate is optimal in the case where f_R or f_L is linear. In the framework of the test case presented in Section 3.3.1, the flux functions are genuinely nonlinear (see Fig. 3b). As it is usual in this case, a convergence of order 1 is observed numerically: see Fig. 11.
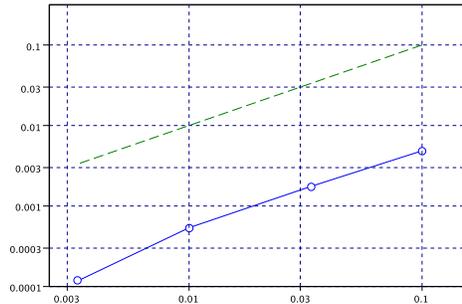

Figure 11: Illustration of the convergence of order 1 in the genuinely nonlinear case. The blue curve correspond to the plot of $\|s_h - s_{\text{ref}}\|_{L^1}$ as a function of Δx, where s_{ref} is a reference solution computed with a small $\Delta x = 10^{-3}$. The green dashed line has a slope equal to 1.

18

Conclusion

The goal of this paper was to investigate the limit, as $\epsilon \to 0$, of the system (15). This study is close to the one performed by E. Kaasschieter [39], but here, we have taken advantage of the recent developments in the theory of the scalar conservation laws with discontinuous flux function (see [20, 7] and references therein) to avoid difficult calculations, and eventually achieved a full classification of possible physical situations. We have identified the correct interface coupling in the discontinuous-flux Buckley-Leverett model in terms of the profiles of the flux functions and capillary pressure functions on two sides from the interface. Moreover, we constructed an adequate numerical method and gave strong evidences on its efficiency.

A Appendix

A.1 The BV_{loc} technique

Let us develop the argument of [18, 20], under the additional assumption that $\varphi_{L,R} \in W^{2,\infty}([0,1])$. Because of the finite speed of propagation and the L^1_{loc} contraction property for $\mathcal{G}$-entropy solutions, completely analogous to the classical estimate of [40], it is enough to prove (31) for an L^1_{loc}-dense subset of initial data. Indeed, a limit of vanishing viscosity limits is still a vanishing viscosity limit.

Thus we pick $s_0 \in C_0^\infty(\mathbb{R})$ and such that $s_0 \equiv 0$ on some interval around zero (this is a way to ensure a smooth transition across the interface $\{x = 0\}$). We extend the corresponding solution s^ϵ of (15) continuously by s_0 for $t \leq 0$; notice that for $t < 0$, the so extended function s^ϵ satisfies

$$\partial_t\big((\phi_L \mathbb{1}_{x<0} + \phi_R \mathbb{1}_{x>0})s^\epsilon\big) + \partial_x\big(f_L(s^\epsilon)\mathbb{1}_{x<0} + f_R(s^\epsilon)\mathbb{1}_{x>0}\big) = \epsilon\partial_x\big(\partial_x\varphi_L(s^\epsilon)\mathbb{1}_{x<0} + \partial_x\varphi_R(s^\epsilon)\mathbb{1}_{x>0}\big) + r(x)$$

where

$$r : x \mapsto \partial_x\Big[\big(f_L(s_0) - \epsilon\partial_x\varphi_L(s_0)\big)\mathbb{1}_{x<0} + \big(f_R(s_0) - \epsilon\partial_x\varphi_R(s_0)\big)\mathbb{1}_{x>0}\Big] \tag{43}$$

is an $L^\infty(\mathbb{R}) \cap L^1(\mathbb{R})$ function, by the assumptions on s_0 and because $f_{L,R}, \varphi_{L,R}$ were assumed regular enough.

Therefore the so extended function s^ϵ is an entire solution (i.e., a solution defined for $t \in \mathbb{R}$) of problem (15) with the additional source term $r(x)\mathbb{1}_{t<0}$. Now, the key fact is that we can control the L^1 time translates of s^ϵ by a linear modulus of continuity, because solutions of (15) with a source term verify the L^1 contraction principle completely analogous to (18):

$$\sum_{i \in \{L,R\}} \int_{\Omega_i} \phi_i|s^\epsilon(t) - s^\epsilon(t-\tau)| \leq \sum_{i \in \{L,R\}} \int_{\Omega_i} \phi_i|s^\epsilon(0) - s^\epsilon(-\tau)| + \int_0^t \int_{\mathbb{R}} |r\,\mathbb{1}_{s<0} - r\,\mathbb{1}_{s-\tau<0}|\,ds = \tau\,\|r\|_{L^1}.$$

Therefore $s^\epsilon \in BV(0,T;L^1(\mathbb{R}))$, with a uniform in ϵ bound. Then we can use the idea of [18, Lemma 4.2] and [20, Lemma 5.4]: for $a > 0$, using the mean-value theorem for each $\epsilon > 0$ we can find a contour $(0,T) \times \{a^\epsilon\}$ with $0 < a^\epsilon < a$ such that $\text{TotVar}\,a^\epsilon$ along these contours is uniformly bounded by $\frac{C}{a}$. The variation of s_0 is also bounded, therefore in the same way as in the classical estimate of Bardos, LeRoux and Nédélec [12] for the Dirichlet problem for viscous conservation law (with boundary datum given by the values of s^ϵ on our contour), we get the bound

$$\text{TotVar}\,s^\epsilon\big|_{\{(t,x)\,|\,t\in(0,T),\,x\geq a\}} \leq \frac{C}{a},$$

with C that only depends on s_0 and on the Lipschitz constant of $f_{L,R}$ and of $\varphi'_{L,R}$. Analogous estimate holds for the variation on the set $\{(t,x)\,|\,t \in (0,T),\,x \leq a\}$. With the Cantor diagonal argument, we deduce compactness of $(s^\epsilon)_\epsilon$ in $L^1_{loc}((0,T) \times \mathbb{R}_+)$ and thus justify (31).

A.2 An asymptotic preserving scheme

As a consequence of Proposition 5 and Theorem 5, we have

$$\lim_{\epsilon \to 0}\left(\lim_{\Delta t, \Delta x \to 0} s_h^\epsilon\right) = s \quad \text{in } L^1_{loc}(\mathbb{R} \times \mathbb{R}_+),$$

where s_h^ϵ is the solution to the scheme (32)–(36). In order to justify the comparison of the numerical solutions s_h^ϵ and s_h on Figures 5,6,8,9,10, we aim to prove that

$$\lim_{\Delta x, \Delta t \to 0}\left(\lim_{\epsilon \to 0} s_h^\epsilon\right) = s \quad \text{in } L^1_{loc}(\mathbb{R} \times \mathbb{R}_+).$$

19

First of all, we need to identify which scheme governs $\lim_{\epsilon \to 0} s_h^\epsilon$.

Lemma 7 *Let s_h^ϵ be the solution of (32)–(36), then $s_h^0 := \lim_{\epsilon \to 0} s_h^\epsilon$ (in the L_{loc}^1 sense) is a solution of the scheme (32)–(36) where ϵ has been set to 0.*

Proof: First of all, since, for all compact subset K of $\mathbb{R} \times \mathbb{R}_+$, the restriction of s_h^ϵ to K lies in a finite dimensional space, the L_{loc}^1 convergence means the convergence of each $s_{j+1/2}^{\epsilon,n}$ ($j \in \mathbb{Z}, n \in \mathbb{N}$) towards some $s_{j+1/2}^{0,n}$. Assume that this holds for $n \in \mathbb{N}$ (this is true for $n = 0$), let us show it for $n+1$.

Since, for all $\epsilon > 0$, $s_{j+1/2}^{\epsilon,n+1} \in [0,1]$, then, up to a subsequence, $s_{j+1/2}^{\epsilon,n+1}$ tends to some $s_{j+1/2}^{0,n+1} \in [0,1]$, and, by a diagonal extraction process, one can assume that this convergence occurs for all $j \in \mathbb{Z}$. Up to an new subsequence, one can assume that $s_{L,R}^{\epsilon,n+1}$ tends to $s_{L,R}^{0,n+1}$ as well as ϵ tends to 0. Note that since the set $\mathcal{P}$ in (20) is closed, $(s_L^{0,n+1}, s_R^{0,n+1}) \in \mathcal{P}$.

For $j \neq 0$, the flux $F_j^{\epsilon,n+1} := G_j(s_{j-1/2}^{\epsilon,n+1}, s_{j+1/2}^{\epsilon,n+1}) - \epsilon \frac{\varphi_j(s_{j+1/2}^{\epsilon,n+1}) - \varphi_j(s_{j-1/2}^{\epsilon,n+1})}{\Delta x}$ satisfies

$$\lim_{\epsilon \to 0} F_j^{\epsilon,n+1} = G_j(s_{j-1/2}^{0,n+1}, s_{j+1/2}^{0,n+1}) := F_j^{0,n+1}.$$

Similarly, it follows from the formulas

$$
\begin{aligned}
F_0^{\epsilon,n+1} &= G_L(s_{-1/2}^{\epsilon,n+1}, s_L^{\epsilon,n+1}) - \epsilon \frac{\varphi_L(s_L^{\epsilon,n+1}) - \varphi_L(s_{-1/2}^{\epsilon,n+1})}{\Delta x/2} \\
&= G_R(s_R^{\epsilon,n+1}, s_{1/2}^{\epsilon,n+1}) - \epsilon \frac{\varphi_R(s_{1/2}^{\epsilon,n+1}) - \varphi_R(s_R^{\epsilon,n+1})}{\Delta x/2},
\end{aligned}
$$

and from the property $(s_L^{0,n+1}, s_R^{0,n+1}) \in \mathcal{P}$, that

$$
\begin{cases}
\tilde{\pi}_L(s_L^{0,n+1}) \cap \tilde{\pi}_R(s_R^{0,n+1}) \neq \emptyset, \\
F_0^{0,n+1} = G_L(s_{-1/2}^{0,n+1}, s_L^{0,n+1}) = G_R(s_R^{0,n+1}, s_{1/2}^{0,n+1}).
\end{cases} \tag{44}
$$

$\square$

The following lemma ensures that the transmission conditions system (44) yields a flux that is well defined.

Lemma 8 *Let $(u_L, u_R) \in [0,1]^2$, then the system*

$$
\begin{cases}
\tilde{\pi}_L(s_L) \cap \tilde{\pi}_R(s_R) \neq \emptyset, \\
F_0^0(u_L, u_R) = G_L(u_L, s_L) = G_R(s_R, u_R)
\end{cases} \tag{45}
$$

admits a least one solution $(s_L, s_R) \in \mathcal{P}$; moreover, the value $F_0^0(u_L, u_R)$ is defined uniquely by (45).

Proof: The set $\mathcal{P}$ can be naturally parametrized by $p \in \bar{\mathbb{R}}$ as follows:

$$\mathcal{P} = \left\{ \left(\tilde{\pi}_L^{-1}(p), \tilde{\pi}_R^{-1}(p) \right) \mid p \in \bar{\mathbb{R}} \right\}.$$

Therefore, finding (s_L, s_R) solution of (45) reduces to finding $p \in \bar{\mathbb{R}}$ such that

$$\Psi_L(p) := G_L(u_L, \tilde{\pi}_L^{-1}(p)) = G_R(\tilde{\pi}_R^{-1}(p), u_R) := \Psi_R(p), \tag{46}$$

where the left-hand side Ψ_L is non-increasing while the right-hand side Ψ_R is non-decreasing. In addition, we have $\Psi_L(-\infty) \geq \Psi_R(-\infty)$ and $\Psi_L(+\infty) \leq \Psi_R(+\infty)$: e.g.,

$$G_L(u_L, 0) \geq G_L(0,0) = 0 = G_R(0,0) \geq G_R(0, u_R)$$

due to the consistency and the monotonicity properties of the numerical fluxes $G_{L,R}(\cdot, \cdot)$. As a consequence, there exists at least one value of p and a unique value of $\Psi_{L,R}(p)$ such that (46) holds. $\square$

In the following proposition, we identify the flux given by (45) with the Godunov flux at the interface, whose explicit formula was derived in [4].

Proposition 9 *Let $(u_L, u_R) \in [0,1]^2$, then the flux $F_0^0(u_L, u_R)$ given by the nonlinear system (45) is equal to the Godunov flux*

$$F_0(u_L, u_R) = \min\left(\bar{F}^\pi, f_L(\min(u_L, \bar{s}_L)), f_R(\max(\bar{s}_R, u_R))\right), \tag{47}$$

where $\bar{F}^\pi = f_{L,R}(s_{L,R}^\pi)$ and (s_L^π, s_R^π) is the connection selected in Section 1.3.

Proof: We perform the proof by a case by case study relying on the resolution of the Riemann problem. First, we need to introduce some notation. Assume that $f_i(u_i) \geq q$ ($i \in \{L, R\}$), then we denote by $u_i^\star$ the unique value of $[0,1]$, called *conjugate* of u_i, such that $f_i(u_i^\star) = f_i(u_i)$ and $(\bar{s}_L - u_i^\star)(\bar{s}_L - u_i) \leq 0$. Moreover, if $f_L(u_L) \leq \bar{F}^{\text{opt}}$ (resp. $f_R(u_R) \leq \bar{F}^{\text{opt}}$), we denote by u_L^R (resp u_R^L) the unique value in $[0,1]$, called *transpose of u_L* (resp. u_R), such that $f_L(u_L) = f_R(u_L^R)$ and $(u_L - \bar{s}_L)(u_L^R - \bar{s}_R) \geq 0$ (resp. $f_R(u_R) = f_L(u_R^L)$ and $(u_R - \bar{s}_R)(u_R^L - \bar{s}_L) \geq 0$). We will denote by $u_L^{R,\star}$ (resp. $u_R^{L,\star}$) the transpose of the conjugate of u_L (resp. u_R) (cf. Fig. 12a). Note that, for $(u_L, u_R) \in \mathcal{U}$, one has $u_R = u_L^{R,\star}$ (and $u_L = u_R^{L,\star}$). In the case where $(u_L, u_R) \in \mathcal{O}$, then either $u_L = u_R^L$ (and $u_R = u_L^R$) if (u_L, u_R) lies on an increasing branch of $\mathcal{O}$, or $u_L = u_R^{L,\star}$ (and $u_R = u_L^{R,\star}$) if (u_L, u_R) lies on the decreasing branch of $\mathcal{O}$. We denote by (s_L^π, s_R^π) the

(a) transpose u_L^R and conjugate $u_L^\star$ of u_L

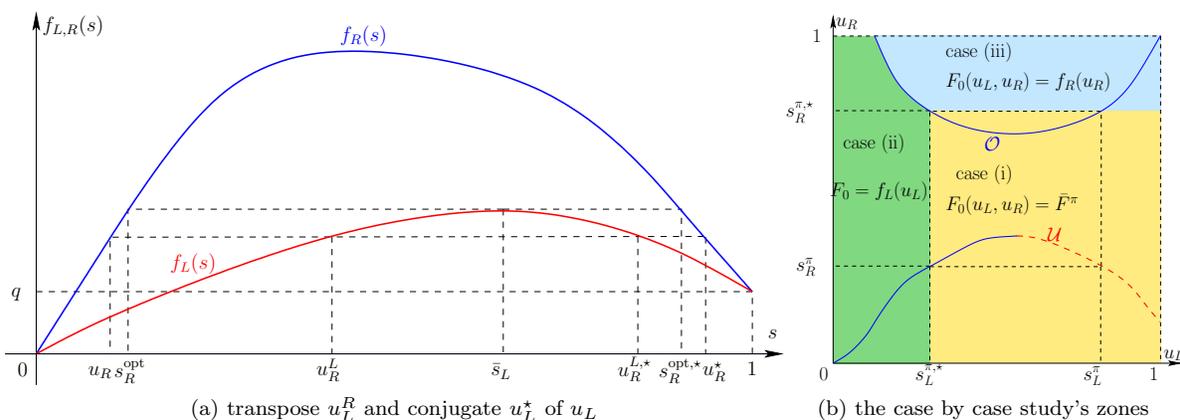(b) the case by case study's zones

Figure 12

connection defined by the Selection Rule at the end of Section 1.3, and by $s_{L,R}^{\pi,\star}$, the conjugate values of $s_{L,R}^\pi$.

(i) Assume first that $u_L \geq s_L^{\pi,\star}$ and $u_R \leq s_R^{\pi,\star}$, then, thanks to Assumption **(A1)**, the Godunov flux given by formula (47) provides $F_0(u_L, u_R) = \bar{F}^\pi$. On the other hand, let us assume that $\mathcal{P} \cap \mathcal{U} \neq \emptyset$, so that $(s_L^\pi, s_R^\pi) \in \mathcal{P}$. From Assumption **(A1)** on the flux functions, we deduce that $G_L(u_L, s_L^\pi) = G_R(u_R, s_R^\pi) = \bar{F}^\pi$. Thus formulas (45) and (47) yield the same value.

(ii) Assume that $u_L \leq s_L^{\pi,\star}$ and that $u_R \leq u_L^{R,\star}$, so that formula (47) provides that the flux at the interface should be given by $F_0(u_L, u_R) = f_L(u_L)$. Let us find a convenient choice of (s_L, s_R) solution to (45) so that $F_0^0(u_L, u_R) = F_0(u_L, u_R)$. The fact that $G_L(u_L, s_L) = G_R(s_R, u_R) = f_L(u_L)$ implies, because of Assumption **(A1)**, that s_L can be chosen arbitrarily in $[0, u_L^\star]$, while s_R has to be equal to u_L^R. Note that $(u_L^\star, u_L^R) \in \mathcal{U}$, and that $u_L^\star \geq s_L^\star$, $u_L^R \leq s_R^\star$. It can thus be seen on Fig. 1 that $([0, u_L^\star] \times \{u_L^R\}) \cap \mathcal{P} \neq \emptyset$. Choosing (s_L, s_R) at this last intersection in (45) ensures that formulas (45) and (47) yield the same value for the flux $F_0(u_L, u_R)$.

(iii) The last case is then $u_R \geq s_R^{\pi,\star}$ and $u_L \geq u_R^{L,\star}$, so that the flux given by (47) turns to be equal to $f_R(u_R)$. From similar argument as in the previous case, we deduce from $G_L(u_L, s_L) = G_R(s_R, u_R)$ that s_R can be chosen arbitrary in $[u_R^\star, 1]$ while the condition $s_L = u_R^L$ is enforced. Here again, the segment $\{u_R^L\} \times [u_R^\star, 1]$ has a non-empty intersection with $\mathcal{P}$. Choosing $(s_L, s_R) \in (\{u_R^L\} \times [u_R^\star, 1]) \cap \mathcal{P}$ ensures that, in this case again, the values given by the formulas (45) and (47) coincide.

The above case by case study is illustrated by Fig. 12b. □

As a direct consequence of formula (47) and of [4], taking $\epsilon = 0$ in the scheme defined by (32)–(36) yields the implicit Godunov scheme corresponding to the notion of $\mathcal{G}_{(s_L^\pi, s_R^\pi)}$-entropy solution. From the monotonicity of the scheme, we deduce that the discrete solution s_h^0 is unique (e.g. [33, 23]). The analysis carried out in [7] for the explicit Godunov scheme can be straightforwardly adapted to the implicit case.

Corollary 10 *Let s_h^0 be the unique approximate solution provided by the scheme* (32)–(36) *in the case $\epsilon = 0$, then*

$$\lim_{\Delta x, \Delta t \to 0} s_h^0 = s \ in \ L_{loc}^1(\mathbb{R} \times \mathbb{R}_+),$$

where s is the unique $\mathcal{G}_{(s_L^\pi, s_R^\pi)}$-entropy solution to the hyperbolic Buckley-Leverett equation in two-rocks' medium.

References

[1] Adimurthi, J. Jaffré, and G. D. Veerappa Gowda. Godunov-type methods for conservation laws with a flux function discontinuous in space. *SIAM J. Numer. Anal.*, 42(1):179–208 (electronic), 2004.

[2] Adimurthi, S. Mishra, and G. D. Veerappa Gowda. Optimal entropy solutions for conservation laws with discontinuous flux-functions. *J. Hyperbolic Differ. Equ.*, 2(4):783–837, 2005.

[3] H. W. Alt, S. Luckhaus, and A. Visintin. On nonstationary flow through porous media. *Ann. Mat. Pura Appl. (4)*, 136:303–316, 1984.

[4] B. Andreianov and C. Cancès. The Godunov scheme for scalar conservation laws with discontinuous bell-shaped flux functions. Submitted.

[5] B. Andreianov, P. Goatin, and N. Seguin. Finite volume schemes for locally constrained conservation laws. *Numer. Math.*, 115(4):609–645, 2010.

[6] B. Andreianov, K.H. Karlsen, and N.H. Risebro. On vanishing viscosity approximation of conservation laws with discontinuous flux. *Networks Het. Media*, 5(3):617–633, 2010.

[7] B. Andreianov, K. Karlsen, and N. Risebro. A theory of L^1-dissipative solvers for scalar conservation laws with discontinuous flux. *Arch. Ration. Mech. Anal.*, pages 1–60, 2011. 10.1007/s00205-010-0389-4.

[8] E. Audusse and B. Perthame. Uniqueness for scalar conservation laws with discontinuous flux via adapted entropies. *Proc. Roy. Soc. Edinburgh Sect. A*, 135(2):253–265, 2005.

[9] K. Aziz and A. Settari. *Petroleum Reservoir Simulation*. Elsevier Applied Science Publishers, Londres, 1979.

[10] F. Bachmann. Analysis of a scalar conservation law with a flux function with discontinuous coefficients. *Adv. Differential Equations*, 9:1317–1338, 2004.

[11] P. Baiti and H. K. Jenssen. Well-posedness for a class of 2×2 conservation laws with L^∞ data. *J. Differ. Equ.* 140(1):161–185, 1997.

[12] C. Bardos, A.-Y. LeRoux, and J.-C. Nédélec. First order quasilinear equations with boundary conditions. *Comm. Partial Differential Equations*, 4(9):1017–1034, 1979.

[13] J. Bear. *Dynamic of Fluids in Porous Media*. American Elsevier, New York, 1972.

[14] M. Bertsch, R. Dal Passo, and C. J. van Duijn. Analysis of oil trapping in porous media flow. *SIAM J. Math. Anal.*, 35(1):245–267 (electronic), 2003.

[15] F. Bouchut and B. Perthame. Kružkov's estimates for scalar conservation laws revisited. *Trans. Amer. Math. Soc.* 350(7):2847–2870, 1998.

[16] K. Brenner, C. Cancès, and D. Hilhorst. Convergence of finite volume approximation for immiscible two-phase flows in porous media with discontinuous capillary pressure field in several dimensions. In preparation.

[17] K. Brenner, C. Cancès, and D. Hilhorst. A convergent finite volume scheme for two-phase flows in porous media with discontinuous capillary pressure field. In *Proceeding of the conference FVCA6*, volume 1, pages 185–193. Springer, 2011.

[18] R. Bürger, A. García, K.H. Karlsen, and J.D. Towers. Difference schemes, entropy solutions, and speedup impulse for an inhomogeneous kinematic traffic flow model. *Netw. Heterog. Media*, 3:1–41, 2008.

[19] R. Bürger, K. H. Karlsen, S. Mishra, and J. D. Towers. On conservation laws with discontinuous flux. In Y. Wang and K. Hutter, editors, *Trends in Applications of Mathematics to Mechanics*, pages 75–84. Shaker Verlag, Aachen, 2005.

[20] R. Bürger, K. H. Karlsen, and J. D. Towers. An Engquist-Osher-type scheme for conservation laws with discontinuous flux adapted to flux connections. *SIAM J. Numer. Anal.*, 47(3):1684–1712, 2009.

[21] F. Buzzi, M. Lenzinger, and B. Schweizer. Interface conditions for degenerate two-phase flow equations in one space dimension. *Analysis*, 29:299–316, 2009.

[22] C. Cancès. Two-phase Flows Involving Discontinuities on the Capillary Pressure In *Proceeding of the conference FVCA5*, pages 249–256. Wiley & Sons, 2008.

[23] C. Cancès. Finite volume scheme for two-phase flow in heterogeneous porous media involving capillary pressure discontinuities. *M2AN Math. Model. Numer. Anal.*, 43:973–1001, 2009.

[24] C. Cancès. Asymptotic behavior of two-phase flows in heterogeneous porous media for capillarity depending only on space. I. Convergence to the optimal entropy solution. *SIAM J. Math. Anal.*, 42(2):946–971, 2010.

[25] C. Cancès. Asymptotic behavior of two-phase flows in heterogeneous porous media for capillarity depending only on space. II. Nonclassical shocks to model oil-trapping. *SIAM J. Math. Anal.*, 42(2):972–995, 2010.

[26] C. Cancès. On the effects of discontinuous capillarities for immiscible two-phase flows in porous media made of several rock-types. *Netw. Heterog. Media*, 5(3):635–647, 2010.

[27] C. Cancès and Th. Gallouët. On the time continuity of entropy solutions. *J. Evol. Equ.* 11(1):43–55, 2011.

[28] C. Cancès, Th. Gallouët, and A. Porretta. Two-phase flows involving capillary barriers in heterogeneous porous media. *Interfaces Free Bound.*, 11(2):239–258, 2009.

[29] C. Cancès and M. Pierre. An existence result for multidimensional immiscible two-phase flows with discontinuous capillary pressure field. hal-00518219, 2010.

[30] C. Cancès and N. Seguin. Error estimate for Godunov approximation of locally constrained conservation laws. hal-00599581, 2011.

[31] R. M. Colombo and P. Goatin. A well posed conservation law with a variable unilateral constraint. *J. Differential Equations*, 234(2):654–675, 2007.

[32] G.-Q. Chen and H. Frid. Divergence-measure fields and hyperbolic conservation laws. *Arch. Rational Mech. Anal.*, 147:89–118, 1999.

[33] R. Eymard, T. Gallouët, and R. Herbin. Finite Volume Methods. *Handbook of Numerical Analysis*, Vol. VII, P. Ciarlet, J.-L. Lions, eds., North-Holland, 2000.

[34] G. Enchéry, R. Eymard, and A. Michel. Numerical approximation of a two-phase flow in a porous medium with discontinuous capillary forces. *SIAM J. Numer. Anal.*, 43(6):2402–2422, 2006.

[35] A. Ern, I. Mozolevski, and L. Schuh. Discontinuous galerkin approximation of two-phase flows in heterogeneous porous media with discontinuous capillary pressures. Submitted, 2009.

[36] B.G. Ersland, M.S. Espedal, and R. Nybo. Numerical methods for flows in a porous medium with internal boundary. *Comput. Geosci.*, 2:217–240, 1998.

[37] T. Gimse and N. H. Risebro. Riemann problems with a discontinuous flux function. *Proceedings of Third International Conference on Hyperbolic Problems*, Vol. I, II (Uppsala, 1990), 488–502, Studentlitteratur, Lund, 1991.

[38] T. Gimse and N. H. Risebro. Solution of the Cauchy problem for a conservation law with a discontinuous flux function. *SIAM J. Math. Anal.*, 23(3):635–648, 1992.

[39] E. F. Kaasschieter. Solving the Buckley-Leverett equation with gravity in a heterogeneous porous medium. *Comput. Geosci.*, 3(1):23–48, 1999.

[40] S. N. Kružkov. First order quasilinear equations with several independent variables. *Mat. Sb.* 81 (123):228–255, 1970.

[41] P.-L. Lions, B. Perthame, and E. Tadmor. A kinetic formulation of multidimensional scalar conservation laws and related equations. *J. Amer. Math. Soc.*, 7(1):169–191, 1994.

[42] M. Maliki and H. Touré. Uniqueness of entropy solutions for nonlinear degenerate parabolic problems. *J. Evol. Equ.*, 3(4):603–622, 2003.

[43] E. Yu. Panov. On sequences of measure valued solutions for a first order quasilinear equation (Russian). *Mat. Sb.*, 185(2):87–106, 1994; Engl. tr. in *Russian Acad. Sci. Sb. Math.*, 81(1):211–227, 1995.

[44] E. Yu. Panov. Existence of strong traces for generalized solutions of multidimensional scalar conservation laws. *J. Hyperbolic Differ. Equ.*, 2(4):885–908, 2005.

[45] E. Yu. Panov. Existence of strong traces for quasi-solutions of multidimensional conservation laws. *J. Hyperbolic Differ. Equ.*, 4(4):729–770, 2007.

[46] E. Yu. Panov. Existence and strong pre-compactness properties for entropy solutions of a first-order quasilinear equation with discontinuous flux. *Arch. Ration. Mech. Anal.*, 195(2), pp.643–673, 2009.

[47] B. Schweizer. Homogenization of degenerate two-phase flow equations with oil trapping. *SIAM J. Math. Anal.*, 39(6):1740–1763, 2008.

[48] D. Serre. *Systems of conservation laws. 2. Geometric structures, oscillations, and initial-boundary value problems* Cambridge University Press, Cambridge, 2000.

[49] C. J. van Duijn, A. Mikelić, and I. S. Pop. Effective equations for two-phase flow with trapping on the micro scale. *SIAM J. Appl. Math.*, 62:1531–1568, 2002.

[50] C. J. van Duijn, J. Molenaar, and M. J. de Neef. The effect of capillary forces on immiscible two-phase flows in heterogeneous porous media. *Transport in Porous Media*, 21:71–93, 1995.

[51] A. Vasseur. Strong traces of multidimensional scalar conservation laws. *Arch. Ration. Mech. Anal.*, 160(3):181–193, 2001.